RESEARCH ON RARE EARTH METALS AND COMPOUNDS AND DEVELOPMENT OF APPLICATIONS BASED ON THEIR MAGNETIC PROPERTIES

Final Technical Report

(2 November 1970 - 1 November 1971)

by

Paul L. Donoho
Franz R. Brotzen
Kamel Salama
L. V. Benningfield

Materials Science Laboratory

Rice University
Houston, Texas 77001

Work performed under Contract No. DAAH01-71-C-0259
Monitored by U.S. Army Missile Command

Sponsored by:

Advanced Research Projects Agency
ARPA Order Nr. 1685

1 December 1971

R 85

Unclassified
Security Classification

DOCUMENT CONTROL DATA - R & D

(Security classification of title, body of abstract and indexing annotation must be entered when the overall report is classified)

1. ORIGINATING ACTIVITY (Corporate author)
Rice University
Materials Science Laboratory
Houston, Texas 77001

2a. REPORT SECURITY CLASSIFICATION
Unclassified

2b. GROUP

3. REPORT TITLE
Research on Rare-Earth Metals and Compounds and Development of Applications Based on Their Magnetic Properties

4. DESCRIPTIVE NOTES (Type of report and inclusive dates)
Final Report 2 November 1970-1 November 1971

5. AUTHOR(S) (First name, middle initial, last name)
Paul L. Donoho, Franz R. Brotzen, Kamel Salama, and
L. V. Benningfield, Jr.

6. REPORT DATE	7a. TOTAL NO. OF PAGES	7b. NO. OF REFS
1 December 1971	75	35

8a. CONTRACT OR GRANT NO.	9a. ORIGINATOR'S REPORT NUMBER(S)
DAAH01-71-C-0259	
b. PROJECT NO.	
c.	9b. OTHER REPORT NO(S) (Any other numbers that may be assigned this report)
d.	

10. DISTRIBUTION STATEMENT
Distribution of this document is unlimited.

11. SUPPLEMENTARY NOTES	12. SPONSORING MILITARY ACTIVITY
	Advanced Research Projects Agency, Arlington, Virginia 22209

13. ABSTRACT

This report describes the technical acomplishments achieved during a one year research program on the magnetic and magnetoelastic properties of materials containing elements of the rare-earth series. A primary goal of this program was the development of highly efficient high-frequency ultrasonic transducers based on the extremely high magnetostriction found in most rare-earth materials. Work has been carried out on the propagation of elastic waves in holmium and terbium single crystals, and results have been obtained for the velocity and attenuation of such waves as functions of the temperature and the strength of an applied magnetic field. Single-crystal transducers of gadolinium and terbium have been constructed, and elastic-wave generation in these transducers has been observed, although only preliminary results have been attained. A new theory of magnetic and magnetoelastic effects in the rare earths has been developed, and it promises to shed new light on these phenomena. A facility for the growth of large single crystals of rare-earth materials has been constructed, making possible the study of a wide range of materials.

DD FORM 1 NOV 68 1473

Unclassified
Security Classification

14 KEY WORDS	LINK A		LINK B		LINK C	
	ROLE	WT	ROLE	WT	ROLE	WT
Rare Earths						
Elements and Compounds						
Magnetic Properties						
Magnetostriction						
Ultrasonic Transducers						
Ultrasonic Propagation						

RESEARCH ON RARE EARTH METALS AND COMPOUNDS AND DEVELOPMENT OF APPLICATIONS BASED ON THEIR MAGNETIC PROPERTIES

Final Technical Report
(2 November 1970 - 1 November 1971)

by

Paul L. Donoho

Franz R. Brotzen

Kamel Salama

L. V. Benningfield

Materials Science Laboratory

Rice University

Houston, Texas 77001

Work performed under Contract No. DAAH01-71-C-0259
Monitored by U.S. Army Missile Command

Sponsored by:

Advanced Research Projects Agency
ARPA Order Nr. 1685

1 December 1971

ABSTRACT

This report describes the technical accomplishments achieved during a one year research program on the magnetic and magnetoelastic properties of materials containing elements of the rare-earth series. A primary goal of this program was the development of highly efficient high-frequency ultrasonic transducers based on the extremely high magnetostriction found in most rare-earth materials. Work has been carried out on the propagation of elastic waves in holmium and terbium single crystals, and results have been obtained for the velocity and attenuation of such waves as functions of the temperature and the strength of an applied magnetic field. Single-crystal transducers of gadolinium and terbium have been constructed, and elastic-wave generation in these transducers has been observed, although only preliminary results have been attained. A new theory of magnetic and magnetoelastic effects in the rare earths has been developed, and it promises to shed new light on these phenomena. A facility for the growth of large single crystals of rare-earth materials has been constructed, making possible the study of a wide range of materials.

TABLE OF CONTENTS

LIST OF FIGURES

LIST OF TABLES

I. INTRODUCTION

This report describes the technical achievements attained in the course of a research program entitled: "Research on Rare-Earth Metals and Compounds and Development of Applications Based on Their Magnetic Properties." This program was sponsored by the Advanced Research Projects Agency, Department of Defense (ARPA Order 1685), and it was administered by the Army Missile Command under Contract No. DAAH01-71-C-0259. The contract performance period was 2 November 1970 through 1 November 1971. This program is being continued for a second year under Contract No. DAAH01-72-C-0286, beginning 5 November, 1971.

The principal emphasis in this research program was directed toward the exploitation of the extremely large magnetostriction of many of the rare-earth elements and compounds for the generation of ultrasonic elastic waves at high intensity and very high frequency. The development of rare-earth magnetostrictive ultrasonic transducers capable of generating extremely intense high-frequency elastic waves will find many applications in such areas as the nondestructive testing of materials, investigation of the nonlinear elastic properties of solids, microwave communications and signal-processing systems, and acoustic holography. In addition to this primary concern of the research described here, the general studies of magnetoelastic phenomena in the rare earths carried out in this program will undoubtedly have important consequences for the development of new permanent-magnet materials, such as the rare-earth cobalt compounds.

The research carried out during the first six months of the contract period has been previously reported in the Semi-Annual Technical Report[1] submitted 1 June 1971 in accordance with contract requirements. Those projects which had been successfully completed during the period covered by the Semi-Annual Report will be mentioned only briefly in this report, in which emphasis is given to projects not completed during the first six months and to new projects initiated during the second half of the contract period.

The research described in this report may be divided into four major areas, and the accomplishments achieved during the contract period may be briefly summarized as follows:

1. The Growth of Single Crystals

Apparatus for the growth of single crystals of the pure rare-earth elements, rare-earth alloys, and rare-earth-transition-group intermetallic compounds was designed, constructed, and successfully operated. This apparatus, which utilizes the induction-heated floating-zone technique for crystal growth, was successfully employed for the growth of large crystals of dysprosium. The quality of the crystals produced with this apparatus is comparable to that of the best crystal previously available to this program. Dysprosium was chosen as the principal material for the initial effort to produce single crystals mainly because it is the least expensive of the magnetically interesting pure rare earths (Gd, Tb, Dy, Ho, Er, Tm) and it

is readily available in the form of rods suitable for the technique employed here. Dysprosium exhibits a solid-state phase transition (bcc-hcp) at a temperature slightly below its melting point and has a rather high vapor pressure at the melting point, two properties which lead to most of the difficulties encountered in attempts to grow single crystals of the rare earths. The success which has been obtained in the case of dysprosium is extremely encouraging, and it is believed that the technique which has been developed in this program can now be successfully applied to the remaining magnetic rare earths and to alloys of these elements with each other. No attempt has yet been made to grow single crystals of the more complicated intermetallic compounds, although preparations have been started to attempt the growth of crystals of the extremely interesting compound $TbFe_2$.

2. Elastic-Wave Propagation in the Rare Earths

The studies of elastic-wave propagation in the pure rare earths, which were reported in detail for the case of terbium in the Semi-Annual Report[1], have been continued and extended to include holmium single crystals. The measurement of elastic-wave attenuation and velocity in the range of several MHz is very important to the primary goal of the program, since the study of the effects of applied magnetic fields on these quantities leads to a better understanding of dynamic magnetoelastic interactions in the rare earths. Furthermore, the results presented here represent the first comprehensive study of the

elastic properties of these materials.

3. Magnetostrictive Generation of Ultrasonic Elastic Waves

Magnetostrictive ultrasonic transducers consisting of thin single-crystal disks of both gadolinium and terbium have been successfully used for the generation and detection of elastic waves in the MHz frequency range. Because single-crystal specimens of the pure rare earths exhibit much greater magnetostriction than do polycrystalline samples, it is expected that they will ultimately perform much better as transducers than do the thin polycrystalline films which were studied earlier and reported upon in the Semi-Annual Report[1]. Consequently, no further work was done on the thin film transducers during the second half of the contract period so that the maximum effort could be directed toward the problems associated with the development of single-crystal transducers. Although the generation of elastic waves by means of magnetostriction was quickly demonstrated in the single-crystal gadolinium and terbium samples, a detailed study of the characteristics of the generation mechanism could not be completed during the contract period. The major problem preventing the acquisition of reliable data was the inadequacy of the ultrasonic spectrometer normally used to generate elastic waves in piezoelectric transducers. This apparatus has

required major modifications to permit the application of a suitable driving signal to the very-low-impedance circuit required to drive magnetostrictive transducers. New equipment ideally suited to the task will, however, be available during the second year of this program.

4. Theory of Magnetic and Magnetoelastic Effects in the Rare Earths

In attempts to explain observations on the generation and the propagation of elastic waves in the pure rare earths, which have been studied in various phases of this research program, it became obvious that much of the theory which has been applied to these problems in the past is inadequate for the explanation of most of the observed effects. This inadequacy stems in part from the understandable attempt to treat crystal-field anisotropy and magnetoelasticity in the case of the rare earths by methods which were appropriate only to the iron-group magnetic materials. By treating the crystal-field contributions to the magnetoelastic Hamiltonian in a more realistic way than the usual effective-field approach, it was possible to see immediately how the more correct approach would explain, at least qualitatively, the results which have been observed. As a further contribution to the theory of magnetic and magnetoelastic effects in the rare earths, a new means of treating dynamic

problems, such as magnetic resonance and ultrasonic generation, has been developed. This new technique, the details of which have not been completely worked out, will permit the interpretation of most of the results obtained thus far, but, more importantly, it will permit a much more intelligent approach to the question of predicting what materials and what methods will yield the best results in attempts to design magnetic or magnetoelastic devices.

In the following sections of this report, the four areas outlined above will be discussed fully, and the results obtained during the contract period, both experimental and theoretical, will be described in detail. The final section of the report summarizes the results of the entire research program during the one-year period of the contract, and it attempts to put the program described here into the context of the overall ARPA Rare-Earth Program and of the other current research on the magnetic properties of the rare earths.

II. THE GROWTH OF SINGLE CRYSTALS

Although the growth of single crystals of the rare earths and their alloys and compounds is not directly related to the primary goals of this research program, the ability to produce a supply of crystals of various compositions and orientations is essential to the overall achievement of those goals within a reasonable period of time. Even though single crystals of the rare earths and some of their alloys are commercially available, delivery times can be quite long, and the cost of such crystals is often very high compared to the cost of high-purity polycrystalline material. Furthermore, in the case of most of the interesting intermetallic compounds, single crystals cannot be obtained at all commercially at the present time. Since nearly all materials containing significant amounts of rare-earth elements are highly anisotropic in their magnetic properties, a fundamental understanding of these properties can usually be obtained only through studies of the properties of single crystals. Thus, a program to permit the growth of single crystals of rare-earth materials of high quality was undertaken at the beginning of this research. Initially, only the pure rare earths were employed in this project, since they are readily available in high-purity polycrystalline form. Success has been achieved in this project in the case of dysprosium, and work has begun on

the magnetostrictively very interesting compound $TbFe_2$.

The growth of single crystals of the rare earths is difficult for several principal reasons:

1. The rare earths are all highly chemically reactive. Most crucible materials interact strongly with the rare earths at temperatures in the vicinity of the melting point. It was decided to overcome this difficulty by the use of the zone-melting technique in the floating-zone configuration.

2. Several of the rare earths exhibit very high vapor pressure at temperatures near the melting point (approximately 1 Torr in the case of dysprosium). This high vapor pressure makes growth impossible in a vacuum, thus ruling out the electron-beam technique. In the present case, it was decided to employ rf induction melting.

3. A most serious problem is the presence in most of the rare earths of allotropic phase transitions at temperatures slightly below the melting point. As is usual in such materials, the existence of such transitions greatly complicates the problem of growing single crystals. In the case of the rare earths, however, the proximity of the transition temperature to the melting point, together with the large temperature gradient which can be maintained in the zone-melting technique, apparently help to overcome the aforementioned difficulties.

As mentioned above, it was decided to employ a floating-zone rf-induction melting technique for the growth of rare-earth crystals. Strain-annealing methods have been employed for this purpose[2-4], but it is usually possible to obtain only crystals of random size and orientation by this method. Other conventional methods of crystal growth have proved unsuccessful[5]. One of the advantages of the zone-melting method is that, if it is successful, single crystals of arbitrary axial length can be produced. Although the diameter of such crystals will always be limited, the shape of the crystals resulting from this method is ideal for many types of magnetic measurement. Several of the rare earths, such as gadolinium and terbium, exhibit vapor pressure at the melting point low enough to permit the use of electron-beam melting in a high vacuum environment, but since the remaining rare earths all have rather high vapor pressures, it was decided to employ rf induction melting in a purified inert-gas atmosphere.

Previous attempts to grow single crystals of the rare earths have been reported by Savitskii et al[6]. For the most part, they employed the strain-anneal method, but they were also successful in growing single crystals of yttrium by the zone-melting technique. Crystals obtained from the Metals Research, Ltd., Cambridge, England, are apparently grown by a zone-melting method, but no details are available concerning their actual technique of growth.

The initial attempt at growing a dysprosium crystal in this research program yielded a rod of 6-mm diameter and 50-mm length containing several sizable single-crystal grains, randomly oriented . This result was obtained with only one pass of the zone thoughout the length of the sample, because the instability of the industrial rf generator made control of the zone length quite difficul.. It was impossible in this initial attempt, therefore, to determine the effects of multiple passes or of the rate of growth. The size of the single-crystal grains was, however, encouraging, since they were all large enough to be used in most of the other experiments being carried out in this program. It was decided, therefore, to modify the rf generator to permit feedback control of the temperature of the molten zone, in order that multiple passes at any rate could be made.

The construction of the mechanical system for the control of the zone position and rotation of the sample during the growth process was rather straightforward. The system was built within a vacuum system originally used for thin-film evaporation. Since the sample rod was to be rotated during growth in order to insure uniformity of the molten zone, it was necessary to provide for motion of the rf induction coil. This coil was fabricated in the form of a three-turn coil wound as a flat spiral, with the first turn soldered to a flat disk. The

disk, through which the sample passed during zone melting, served to concentrate the rf magnetic field so that a molten zone of minimum length could be produced. The induction coil could be translated along the sample axis at speeds up to 100 cm/hr. The coil-sample arrangement is shown in Fig. 1. The apparatus was enclosed within a belljar which could be evacuated to high vacuum. The belljar could be outgassed by means of a heating mantle, and, after overnight pumping, an ultimate vacuum pressure of 1.0×10^{-7} could normally achieved.

Because of the high vapor pressure of most of the rare-earth materials, crystal growth was carried out in a helium atmosphere. After overnight bakeout of the system at high vacuum, a thin film of the specimen material was deposited over the belljar. The vacuum pump was then isolated from the belljar, and helium gas was introduced into the chamber. This gas was purified by passing it over a heated rare-earth specimen and through a liquid-nitrogen trap. The final pressure in the belljar prior to commencement of the crystal growth was approximately 500 Torr.

As mentioned above, the most serious problem in the actual zone-melting process is the control of the zone temperature. This problem is illustrated in Fig. 2, in which a dysprosium sample which was zone-melted with poor control is compared with one obtained with good temperature control. Adequate control of the rf output of the induction generator was achieved by

means of a saturable reactor placed in series with the primary side of the high-voltage transformer of the gnerator. A small control signal permits variation of the output power from zero to its maximum value, and the output is easily stabilized by means of a feedback signal proportional to the output current. With the very stable output power obtained in this manner from the gen rator, a uniform zone could be maintained with manual control of the power level.

An attempt was made initially to fabricate dysprosium rods of 6-mm diameter and 10 to 15 cm length by induction melting of high-purity material in a water-cooled copper crucible. It proved, however, difficult to obtain rods of uniform cross section by this means, and this method was, therefore, abandoned. Uniform cast rods of vacuum-distilled dysprosium (and of the other magnetic rare earths) were obtained from Research Chemicals, Inc., Phoenix, Arizona. These rods, 6 mm in diameter and 10 cm in length, were cast in a tantalum crucible, and the impurity levels quoted by the vendor were the following:

Y	0.01	%	Mg	0.005	%	Gd	0.01	%	Ta 0.3 %
Tm	0.01	%	Si	0.001	%	Er	0.01	%	Gaseous Ele-
Yb	0.001	%	Fe	0.005	%	Ho	0.01	%	ments Unknown
Ca	0.02	%	Sm	0.01	%	Tb	0.01	%	

Since it was stated by the vendor that most of the tantalum in the rods was probably on the surface, the rods were etched and electropolished in a solution of 1.0 % perchloric acid in methanol.

The rods were then used in the zone-melting apparatus, and, because of their uniform cross section and density, it was possible to obtain fairly uniform melting on even the first pass. Three or four passes were made in most cases at a speed of approximately 4 cm/hr. Upon examination, after etching the samples in the perchloric acid-methanol solution, several grains could be seen on the outer surface, typically 1-3 mm in width and 3-15 mm in length. A section taken from the center of the zone-melted region, revealed typically, however, a large interior single-crystal region (60% of the cross-sectional area) with small grains around the circumference. A longitudinal section revealed that the large central single-crystal region extended several centimeters along the rod axis.

It was decided to anneal the specimen containing the largest of these single-crystal regions in a sealed tantalum crucible, and this process was carried out at a temperature of 1300° C for 66 hr. Subsequent analysis of the sample revealed that the central single-crystal region had grown to occupy the full 5-cm length of the rod, although there were still several small grains around the circumference. The average cross-sectional fraction occupied by the single crystal was, however, estimated to be greater than 75% after the anneal.

X-ray analysis, using back-reflection techniques,

showed no evidence of a mosaic structure or of other major lattice defects. The overall quality of the X-ray results was comparable to that of the best previous crystals available in this laboratory.

The problems associated with the growth of single crystals of the rare earths have not been entirely solved, but the success which has been achieved during the contract period is encouraging. Crystals as large as any which were previously available have been grown, and their quality is more than adequate for most of the experiments associated with this research program. Work in this area will continue, and it is believed that a reasonably complete characterization of the crystals produced in this apparatus will be obtained shortly. New problems will undoubtedly be encountered in the case of the intermetallic compounds, such as $TbFe_2$, currently the most interesting of these compounds from the point of view of this program, but work is in progress to attempt the growth of this and other materials, and these problems should soon be revealed.

III. ELASTIC-WAVE PROPAGATION IN THE RARE EARTHS

Studies of elastic-wave propagation in rare-earth single crystals provide considerable insight into the nature of the magnetoelastic interaction in these materials. In fact, the study of the velocity and attenuation of high-frequency elastic waves, and particularly the study of the dependence of these quantities on the value of an applied magnetic field, provides information having a direct bearing on the phenomena whose study is one of the primary goals of this program: the magnetostrictive generation of high-frequency elastic waves[7,8]. Furthermore, the knowledge of the values of the elastic constants obtained from measurement of the elastic-wave velocities, is important not only in the analysis of magnetoelastic properties of the rare earths but also for other technological applications of these materials. The work described here has included the determination of the elastic constants of the elements terbium and holmium as well as the determination of the magnetic-field and temperature dependences of elastic-wave attenuation in these elements.

A. The Elastic Constants of Terbium and Holmium

1. Background:

The heavy rare-earth metals undergo magnetic phase transitions at temperatures in the cryogenic range, with the

exception of gadolinium, whose Curie temperature is 293 K. In terbium, a paramagnetic-helimagnetic transition occurs at 229 K, and a helimagnetic-ferromagnetic transition occurs at 221 K. The neutron-diffraction studies of Koehler et al[9,10] revealed that in the helimagnetic state, the magnetization in each basal plane is uniform, and that the magnetization direction varies from plane to plane in a helical manner, the interlayer turn angle varying from 20.5° at 229 K (the Neel temperature, T_N) to 18.5° at 221 K (the Curie temperature, T_C). Below T_C, terbium is a simple ferromagnet with the magnetization lying in the basal plane. These magnetic transitions, particularly the first-order transition at T_C, which is accompanied by a magnetostrictive structural change, can be expected to have a significant effect on the elastic properties of the material, and, indeed, anomalies in the isotropic elastic moduli of both terbium and holmium have been previously reported at temperatures near the magnetic phase transitions[11].

Similar to the case of terbium, holmium undergoes two major phase transitions. There is a paramagnetic-helimagnetic transition at T_N= 131 K, with a helimagnetic-ferromagnetic transition at T_C= 20 K. Again, this structure was established by neutron-diffraction studies[12,13], which revealed that the ferromagnetic state has a conical magnetization structure, with a helical interlayer variation, but with a uniform projection of

of the magnetization along the hexagonal axis. From 20 K to 35 K the helical structure is highly distorted, and the application of a strong magnetic field in the helimagnetic range leads to the establishment of several complex ordering structures.

Several of the elastic constants of dysprosium[14] and gadolinium[15,16] have been reported, but a complete set of values for the elastic constants of terbium and holmium has not previously been available. Only the velocities of ultrasonic longitudinal and shear waves propagating along the c-axis have been reported in connection with attenuation measurements[17,18].

2. Sample Preparation and Experimental Procedure:

Single crystals of terbium and holmium were obtained from Metals Research, Ltd., Cambridge, England, in the form of cylinders 6 mm in diameter. These crystals were spark-cut to a length of approximately 6 mm and electro-polished so that the faces were parallel within a fraction of one degree. Three samples were required of each of the elements for this investigation:

(1) a crystal having two parallel surfaces normal to the c-axis [0001];

(2) a crystal having two surfaces normal to the b-axis $[10\bar{1}0]$;

(3) a crystal having two parallel surfaces at a 45° angle between the c-plane and the b-plane.

The samples were electropolished to remove surface layers, and their orientation was determined by means of Laue back-reflection X-rays to within 2° of the desired orientation.

Measurements of the elastic-wave velocities were carried out by the pulse-superposition method of Mc Skimin[19]. The experimental arrangement used in this method is shown schematically in Fig. 3. Pulses of approximately 1-μsec duration and of varying pulse repetition rate were generated with a tone-burst generator and applied to the quartz transducer. The transducers used in this work included both X-cut and Y-cut quartz crystals with a 20-MHz fundamental resonance. These transducers were supplied by the Valpey Corp., Holliston, Mass. The transducers were bonded to the experimental samples with Dow-Corning 276-V9 fluid. In cases when the attenuation was quite large, other bonds were tried, but they failed to yield improved results. The reflected echoes were amplified and displayed without rectification on an oscilloscope, and the repetition rate was adjusted until the echoes from successive pulses were in phase. This technique permits extremely accurate measurement of the wave velocity.

The relationships between the elastic constants and the wave velocities for all the crystallographic orientations employed here are given in Table I. For the calculation of these constants, the following densities were used[20]:

Tb: $\rho = 8.272$ g/cm^3, and Ho: $\rho = 8.803$ g/cm^3. These densities were not corrected for temperature variations in view of the relatively low thermal-expansion coefficients of these metals.

3. Results and Discussion

The elastic constants obtained in this investigation are compiled in Table II for terbium and in Table III for holmium. The constants c_{33} and c_{44} were determined directly from measurements in the [0001] crystals. The constant c_{11} was obtained directly from measurements in the [10$\bar{1}$0] crystal, but in the case of terbium the attenuation of the longitudinal waves in this crystal was so high at temperatures below T_C that sufficiently strong echoes were not observable. The values for c_1 in terbium between T_C and 150 K were, therefore, calculated from the measured quasilongitudinal and quasishear velocities, v_{QL} and v_{QS} (cf. Table I), using also the directly determined values of c_{33} and c_{44}. In both holmium and terbium, the velocity v_4, together with the value determined for c_{11}, permitted the determination of c_{12}. The proper combination of v_{QL} and v_{QS}, together with utilization of c_{33} and c_{44} yielded the value of the elastic constant c_{13}. Tables II and III also tabulate the normal compressibilities of the two elements. The formula used in the calculation of these compressibilities is given in a footnote to Table II.

The tabulated results for terbium are also shown in

TABLE I. Relation between Measured Sound Velocities and Elastic Constants.

Velocity		Crystal Axis	Displacement Direction	Relation
(a)	v_1	[0001]	[0001]	$\rho v_1^2 = c_{33}$
(b)	v_2	[0001]	Any direction in the (0001).	$\rho v_2^2 = c_{44}$
(c)	v_3	$[10\bar{1}0]$	$[10\bar{1}0]$	$\rho v_3^2 = c_{11}$
(d)	v_4	$[10\bar{1}0]$	$[\bar{1}2\bar{1}0]$	$\rho v_4^2 = c_{66} = \frac{1}{2}(c_{11} - c_{12})$
(e)	v_{QL}	Quasilongitudinal along an axis 45° between [0001] and $[10\bar{1}0]$		$\rho v_{QL}^2 = \frac{1}{4}(c_{11} + c_{33} + 2c_{44}) + \frac{1}{2}[\frac{1}{4}(c_{11} - c_{33})^2 + (c_{13}+c_{44})^2]^{\frac{1}{2}}$
(f)	v_{QS}	Quasishear along an axis 45° between [0001] and $[10\bar{1}0]$		$\rho v_{QS}^2 = \frac{1}{4}(c_{11} + c_{33} + 2c_{44}) - \frac{1}{2}[\frac{1}{4}(c_{11} - c_{33})^2 + (c_{13}+c_{44})^2]^{\frac{1}{2}}$

TABLE II. The Elastic Constants of Terbium.*

Temp. K	c_{33} (1)	c_{44} (2)	c_{11} (3)	c_{12} (4)	c_{13} (5)	K (6)	K (7)	K_V (8)
80	7.983	2.385						
90	7.948	2.381						
100	7.917	2.373						
110	7.875	2.364						
120	7.828	2.353						
130	7.783	2.344						
140	7.735	2.335						
150	7.680	2.321	6.561	1.847	1.997	0.0780	0.1004	0.2788
160	7.620	2.303	6.603	1.917	2.048	0.0783	0.0986	0.2755
170	7.550	2.284	6.661	2.015	2.108	0.0786	0.0961	0.2716
180	7.488	2.265	6.731	2.103	2.165	0.0792	0.0940	0.2672
190	7.390	2.246	6.819	2.251	2.223	0.0809	0.0904	0.2672
200	7.295	2.227	6.929	2.399	2.273	0.0829	0.0870	0.2569
210	7.155	2.210	7.085	2.555	2.311	0.0860	0.0833	0.2524
215	7.080	2.204	7.165	2.625	2.321	0.0874	0.0816	0.2509
220	7.070	2.206	7.186	2.704	2.318	0.0886	0.0806	0.2498
225	7.015	2.106	7.183	2.751	2.315	0.0901	0.0797	0.2495
227	6.870	2.193	7.170	2.730	2.312	0.0903	0.0793	0.2497
230	7.018	2.189	7.149	2.683	2.312	0.0894	0.0805	0.2504
240	7.160	2.181	7.017	2.531	2.308	0.0855	0.0841	0.2537
250	7.195	2.174	6.957	2.491	2.306	0.0844	0.0853	0.2550
260	7.210	2.166	6.909	2.463	2.305	0.0836	0.0861	0.2558
270	7.215	2.160	6.875	2.451	2.301	0 0833	0.0867	0.2567
280	7.220	2.153	6.837	2.451	2.299	0.0832	0.0872	0.2572
290	7.225	2.147	6.810	2.430	2.299	0.0826	0.0877	0.2580
300	7.225	2.140	6.788	2.432	2.299	0.0825	0.0879	0.2583

(1) Using relation (a), Table I.
(2) Using relation (b), Table I.
(3) Using relations (e) and (f), Table I, and (1) and (2), Table II.
(4) Using relation (d), Table I, and (3), Table II.
(5) Using relation (e), Table I, and (1), (2), (3), and (4), Table II.

(6) $$K = \frac{c_{11} + c_{12} - 2c_{13}}{c_{33}(c_{11} + c_{12}) - 2c_{13}^2}$$

(7) $$K = \frac{c_{33} - c_{13}}{c_{33}(c_{11} + c_{12}) - 2c_{13}^2}$$

(8) $$K_V = K + 2K$$

*The elastic constants, (1) through (5), are given in units of 10^{11} dyne/cm^2; the compressibilities, (6) through (8), are given in units of 10^{-11} cm^2/dyne.

TABLE III. The Elastic Constants of Holmium.*

Temp. K	(1) c_{33}	(2) c_{44}	(3) c_{11}	(4) c_{12}	(5) c_{13}	(6) K	(7) K	(8) K_V
80	8.084	2.922	8.125		2.048			
90	8.033	2.885	8.081		2.052			
100	7.982	2.847	8.035		2.055			
110	7.930	2.809	7.993		2.060			
120	7.879	2.772	7.950	2.538	2.059	0.0859	0.0785	0.2429
125	7.852	2.754	7.942	2.580	2.123	0.0853	0.0778	0.2409
130	7.828	2.748	4.935	2.627	2.083	0.0854	0.0776	0.2416
135	8.056	2.746	7.922	2.654	2.076	0.0839	0.0781	0.2400
140	8.085	2.742	7.913	2.653	2.071	0.0836	0.0783	0.2400
150	8.107	2.734	7.893	2.649	2.067	0.0833	0.0785	0.2404
160	8.116	2.725	7.875	2.647	2.065	0.0832	0.0787	0.2406
170	8.118	2.716	7.857	2.643	2.063	0.0831	0.0789	0.2409
180	8.117	2.709	7.838	2.640	2.059	0.0831	0.0791	0.2413
190	8.112	2.700	7.817	2.635	2.057	0.0831	0.0793	0.2417
200	8.107	2.692	7.798	2.630	2.057	0.0830	0.0795	0.2420
210	8.101	2.684	7.780	2.628	2.056	0.0830	0.0797	0.2424
220	8.093	2.675	7.762	2.625	2.055	0.0830	0.0798	0.2427
230	8.085	2.668	7.742	2.622	2.053	0.0830	0.0800	0.2431
240	8.076	2.659	7.725	2.619	2.056	0.0830	0.0802	0.2437
250	8.067	2.650	7.705	2.615	2.056	0.0830	0.0804	0.2437
260	8.058	2.639	7.686	2.612	2.059	0.0830	0.0805	0.2440
270	8.048	2.627	7.668	2.610	2.062	0.0829	0.0807	0.2442
280	8.038	2.616	7.650	2.606	2.063	0.0829	0.0808	0.2446
290	8.027	2.604	7.631	2.603	2.063	0.0829	0.0810	0.2449
300	8.015	2.592	7.612	2.600	2.072	0.0828	0.0811	0.2451

* The elastic constants, (1) through (5), are given in units of 10^{11} dyne/cm^2; the compressibilities, (6) through (8), are given in units of 10^{-11} cm^2/dyne.

graphic form in Figs. 4 through 8. In the paramagnetic phase, the elastic constants have a general tendency to increase with decreasing temperature. In the case of c_{33} and c_{66}, a sharp minimum is observed in the region of the magnetic transitions, Figs. 4 and 5. Rosen and Klimker[14] observed a similar minimum at T_N for c_{33} in dysprosium, and all three elastic constants in chromium display the same behavior at T_N. In contrast, the constants c_{12} and c_{13} in terbium, shown in Fig. 7, reach a maximum value near T_N, and this also appears to be the case for c_{11}, Fig. 6.

The error in the constants whose values were obtained directly from the measured velocities is estimated to be less than 1 %, but the error may reach 3 % in the cases of the elastic constants which were determined indirectly. The special difficulty in the determination of c_{11} directly from the wave velocity below T_C is brought out in Fig. 6. The difference between the results for c_{11} obtained directly and indirectly probably indicates that the magnetoelastic interaction at high frequency depends on the wave propagation and polarization vectors. Such dependence was observed also in the case of chromium[21], where the values for the constant c_{44} determined from the wave velocity in the [100] direction differed substantially from those obtained by measuring the velocity in the [110] direction.

The elastic-wave velocities in terbium measured at

different temperatures are given in Table IV. The listed values were obtained from smooth curves of the velocities as functions of the temperature. An analysis of the velocities of the longitudinal waves along the c-axis in the paramagnetic phase near T_N reveals that they follow a logarithmic function of the reduced temperature, as shown also in Fig. 9:

$$\frac{\Delta v_\ell}{v_\ell} = -K \ln \left[\frac{T - T_N}{T_N} \right] \qquad (1)$$

This rather weak temperature dependence is in agreement with theory[18].

The observation that Eq. (1) is obeyed by the results is taken as an indication for the predominance of a single relaxation process in the vicinity of T_N, presumably a spin-phonon interaction. The relaxation time of this process, τ, can be computed from the equation[22]

$$\tau = \frac{v_\ell}{\omega^2} \cdot \Delta\alpha / (-\Delta v_\ell / v_\ell)$$

In this equation, $\Delta v_\ell / v_\ell$ is measured at T_N, and $\Delta\alpha$ denotes the difference in the attenuation coefficient between the paramagnetic state far from T_N and its value at T_N. The value for $\Delta\alpha = 0.21\ cm^{-1}$, determined in this work, leads to a value for the relaxation rate $1/\tau = 6 \times 10^9\ sec^{-1}$, comparable to the rate $7 \times 10^9\ sec^{-1}$ obtained by Luthi et al[18].

The temperature dependences of the elastic constants of holmium are shown in Figs. 10 through 13. With the exception

TABLE IV. The Ultrasonic Velocities in Terbium.*

Temp K	v_1	v_2	v_3	v_4	v_{QL}	v_{QS}
80	3.106	1.698		1.713		
90	3.099	1.696		1.712		
100	3.094	1.694		1.708	2.945	
110	3.085	1.691		1.705	2.933	
120	3.078	1.687		1.701	2.921	
130	3.067	1.683		1.697	2.909	
140	3.058	1.680		1.692	2.903	
150	3.048	1.675		1.688	2.899	1.735
160	3.035	1.668		1.682	2.897	1.729
170	3.023	1.661		1.675	2.895	1.722
180	3.009	1.654		1.669	2.895	1.716
190	2.989	1.647		1.662	2.894	1.712
200	2.968	1.641		1.654	2.894	1.708
205	2.958	1.638		1.650	2.894	1.704
210	2.941	1.635		1.647	2.894	1.705
216	2.923	1.632		1.642	2.893	1.703
218	2.916	1.633		1.641	2.893	
220	2.922	1.633		1.640	2.893	1.702
221			2.879			
222	2.917	1.632	2.888	1.640	2.890	
224	2.909	1.630	2.893	1.638	2.889	
226	2.894	1.629	2.889	1.635	2.888	1.700
227	2.882		2.899	1.625		
228	2.895	1.628	2.892	1.640	2.887	
230	2.912	1.627	2.896	1.647	2.887	1.699
231			2.899			
235	2.932	1.625	2.890	1.648	2.885	1.701
240	2.942	1.624	2.891	1.646	2.884	1.699
245	2.947	1.623	2.888	1.645	2.883	1.698
250	2.950	1.621	2.884	1.643	2.881	1.697
260	2.953	1.618	2.878	1.639	2.879	1.693
240	2.954	1.616	2.874	1.635	2.876	1.691
280	2.954	1.613	2.871	1.631	2.873	1.688
290	2.955	1.611	2.866	1.627	2.870	1.685
300	2.956	1.609	2.864	1.623	2.868	1.683

* The velocities are given in units of 10^5 cm/sec.

For explanation of the symbols used for the velocities see Table I.

of c_{13}, the constants all exhibit normal behavior in the paramagnetic phase. As T_N is approached, the constants undergo changes, the largest of which was observed in c_{33}, Fig. 10. In this case the decrease reaches a value of 4 % and is characteristic of a second-order phase transition.

The compressibilities are shown in Fig. 14 as functions of the temperature. These compressibilities were calculated from the elastic-constant values given in Table III. It is noteworthy that the changes in the compressibilities of holmium at T_N are rather small compared to those observed in terbium, Fig 8. This difference can be attributed to a large variation of the compressibilities near the Curie temperature and a relatively small one near the Néel temperature. This behavior was actually observed in the case of dysprosium by Rosen and Klimker[14]. The large variation in holmium at T_C was not observed in the work reported here, since T_C = 20K, and the measurements given here extends only as low as 78 K. In terbium, however, the helimagnetic phase extends over a temperature range of only 8 degrees, so that the effects of the two phase transitions on the two compressibilities overlap.

A knowledge of the elastic constants makes a calculation of the Debye temperature feasible. By the method of direct integration for hexagonal crystals[23], using the elastic constants measured at 300 K listed in Table II, the Debye

temperature for terbium was found to be 176.6 K. This is in good agreement with the value 174 K computed by Rosen[24] from the elastic moduli of polycrystalline terbium. Both these values are, however, higher than the calorimetrically determined value of 158 K[25]. Calculation of the Debye temperature for holmium by the same method yielded a value of 181 K, which is in agreement with the value 184 K obtained from the moduli of polycrystalline holmium[24]. As in the case of terbium, the computed values exceed the value of 161 K which has been dtermined from specific-heat data[25].

B. The Attenuation of Ultrasonic Elastic Waves in Terbium and Holmium

Changes in the elastic-wave attenuation are quite marked near the magnetic phase transitions in the heavy rare earths. The variation of this attenuation with the intensity of an applied magnetic field generates valuable information concerning the magnetoelastic interactions in these materials. In fact, the attenuation is directly related to those magnetoelastic properties which are most important for the generation of elastic waves through the magnetoelastic interaction. The results of the measurement of elastic-wave attenuation in terbium were presented in detail in the Semi-Annual Report[1]. Additional work was carried out in this area during the second half of the

contract period, and measurements on the attenuation in holmium were begun. These results are summarized here.

1. Effect of Magnetic Field on Elastic-Wave Propagation in Terbium:

In order to measure the attenuation of elastic waves in terbium, essentially the same apparatus was used as that employed in the measurement of velocity. The cryostat was installed in such a way that the sample was in the gap of a large electromagnet capable of producing a uniform field as high as 17 kG. The measurements on terbium were made in the temperature range from 280 K to 180 K, which includes the paramagnetic, helimagnetic, and ferromagnetic phases of terbium. The magnetic field was always parallel to the basal plane, and it was parallel to either the a-axis or the b-axis.

Figures 15 and 16 show the temperature dependence of the first reflected echo amplitude in the presence of a magnetic field. At zero magnetic field, the echo amplitude decreases sharply as the transition into the helimagnetic phase is approached, and it then decreases more slowly to exhibit a minimum at T_C, with a shoulder at T_N. In the presence of a magnetic field, both the amplitude of the minimum and its position on the temperature scale are affected. At small values of the applied field, the amplitude of the minimum increases with

increasing field until the echoes disappear completely at a field of 2 kOe (the field is always given in terms of the applied field, since the sample geometry precluded the use of a simple demagnetizing factor to permit the calculation of the internal field). An increase in the magnetic field beyond this level leads to a decrease in the amplitude of the minimum. The position of the minimum is always shifted to higher temperature as the field is increased; this shift is largest when the field is applied along the a-axis.

Figure 15 illustrates the dependence of the temperature at which the minimum echo amplitude occurs on the magnetic-field intensity for both the a- and b-axis cases. From this figure, it can be seen that the data points for each case lie on a straight line. The slope of the line representing the a-axis data is greater than that for the b-axis case. The intercept of both lines with the temperature scale at $H = 0$ lies at $T = 228.5$ K, approximately the value of T_N. The difference in the slope of the two lines is undoubtedly the result of the basal-plane magnetocrystalline anisotropy.

In order to compare the results shown in Figs. 15 and 16 with existing theories, the attenuation, rather than the echo amplitude, must be accurately determined. This determination could not be made in the many cases where only one echo could be observed or, of course, in cases where the attenuation becomes

so large that the entire echo pattern disappears. In the extreme field limits, namely H = 0 and H = 15 kOe, reproducible attenuation measurements could be made. These results are shown in Fig. 18.

Several theories have been developed to interpret elastic-wave attenuation at magnetic phase transitions[26-31]. All of these theories are based on a critical scattering mechanism at the phase transition, and it should be observed that this mechanism is probably inoperative at temperatures well removed from the phase transitions in the rare earths. The existing theories all lead to the same form for the expected dependence of the attenuation of longitudinal waves on wave number, q, and reduced temperature, $\epsilon = (T - T_N)/T_N$:

$$\alpha_\ell(q, \epsilon) = Bq^2 \epsilon^{-\eta} , \qquad (3)$$

where B is a temperature-independent constant from which the magnetoelastic coupling can be determined, and η is an exponent which characterizes the spin-fluctuation mechanism responsible for the magnetic transition.

In order to compare the experimental results shown in Fig. 18 with Eq. (3), the temperature-independent contribution to the attenuation was considered to be constant, and it was subtracted from the measured values to give the contribution pertinent to the theory. Figure 18 gives a log-log plot of the

attenuation versus $T-T_p$, where T_p is the position of the attenuation peak on the temperature scale. From this figure, it can be seen that, in the absence of a magnetic field, a straight line represents a good fit to the data. In the case of an appreciable applied field, however, two power-law regions characterize the results. In each region, the exponent is independent of the direction of the magnetic field. Furthermore, the exponent of the high-temperature power law is equal to the exponent which applies at zero magnetic field. In the low-temperature region, both B and η are much smaller than in the high-temperature region.

The values for the constants B and η in Equation (3) obtained in this work are compared below with the values experimentally obtained by Pollina and Luthi[32] and with whose calculated by Laramore and Kadanoff[31]:

EXPONENT η

Applied Field	Present Investigation High Temp.	Low Temp.	P. and L.[32]	L. and K.[31]
0	1.45 ± 0.2		1.24 ± 0.1	3/2 or 4/3
15 kOe	1.45 ± 0.2	0.32 ± 0.1		

CONSTANT B

0	1.4×10^{-9}		1.2×10^{-9}	4.7×10^{-9}
15 kOe (a-axis)	5.1×10^{-9}	2.3×10^{-7}		
15 kOe (b-axis)	10.0×10^{-9}	2.6×10^{-7}		

2. Attenuation of Elastic Waves in Holmium:

Attenuation measurements in holmium have not yet been completed. The attenuation of 20 MHz longitudinal waves propagating along the hexagonal axis has been measured in the temperature range from 300 K to 78 K, with the results shown in Fig 20. It can be seen that the attenuation decreases slowly with decreasing temperature, but that it begins to rise sharply as the helimagnetic phase transition is approached. Below T_N, the attenuation again decreases to a value near the high-temperature value. This peak was observed previously by Pollina and Lüthi[32] at frequencies from 50 MHz to 170 MHz.

The effect of an applied magnetic field on the attenuation of c-axis longitudinal waves in holmium was also investigated in the temperature range from 4.2 K to 300 K. The field was applied in the basal plane along the a- or b-axis. In the temperature range between 300 K and 70 K, where quantitative measurements were possible, no effect of the magnetic field could be observed up to an intensity of 18 kOe, nor was any effect observed down to 35 K, although quantitative measurements were impossible in this range. This behavior is, of course, contrary to what was found in terbium, where the effects of applied magnetic fields are very strong, even at temperatures well above the transition temperature, T_N.

Below 35 K, and, in particular, below 20 K, T_C, the effect

of the applied field is observable, although accurate measurements have not yet been possible. Work is proceeding in this area, and it is hoped that some light can be shed on the strikingly different behavior of holmium, compared to terbium, when measurements are made with different crystal orientations and with shear as well as longitudinal waves.

IV. ELASTIC-WAVE GENERATION IN MAGNETOSTRICTIVE RARE-EARTH TRANSDUCERS

In the Semi-Annual Report[1] covering the first six months of the contract period, the work which had been carried out on the generation of elastic waves in thin-film polycrystalline magnetostrictive transducers of various rare earths was reported in detail. The emphasis during the remainder of the contract period has been placed on the generation of elastic waves in single-crystal transducers. Although the single-crystal transducers should exhibit higher efficiencies in the generation of elastic waves at high frequencies than do the polycrystalline thin films, certain experimental problems have prevented a thorough study of this generation in such single-crystal transducers during the period of interest. Elastic-wave generation has been observed at frequencies of 3-10 MHz in transducers of gadolinium and terbium, in the form of thin single-crystal disks, but the dependence of the amplitude of the generated waves on both temperature and applied magnetic field is quite complex. Both longitudinal and transverse waves are generated with different temperature and field dependences. Several major problems arose during the measurement of the elastic-wave amplitudes in this work, however, and the data obtained are not sufficient at this time to permit a satisfactory interpretation. The results obtained up to the present are, therefore, summarized in this

report, together with a description of the improvements which are planned to the experimental technique. These improvements will make both the acquisition and the interpretation of data much simpler.

In the case of both gadolinium and terbium, elastic-wave generation has been observed in single-crystal magnetostrictive transducers at temperatures from the ordering temperatures (T_C = 293 K for Gd, and T_N = 229 K for Tb) down to 77 K, at frequencies in the range of several MHz. Both longitudinal and transverse waves were observed, but the dependence of their amplitude on field and temperature agrees with expectations only in the case of terbium in the ferromagnetic phase. In this case, the generation of elastic waves exhibits a resonant behavior with a resonant value of the magnetic field whose temperature dependence follows the same type of curve as that observed by Blackstead and Donoho[33] for ferromagnetic resonance in dysprosium. The resonant field increases with decreasing temperature below the Curie temperature until it reaches a maximum value at a temperature equal to approximately two-thirds the Curie temperature. The value of the resonant field then remains constant as the temperature is further decreased. This behavior is obtained only with the applied field along a hard magnetization direction in the basal plane (the a-axis, in the case of Tb) and with the driving rf magnetic field along an easy direction (the b-axis, in the case of Tb). This behavior, although similar to the case

of ferromagnetic resonance in dysprosium, is totally unpredicted by current theory[34], and it has helped to stimulate the theoretical work on the dynamic magnetic and magnetoelastic properties of the rare earths reported in the following section of this report.

The work in this area has been hampered by the nature of the apparatus available for the generation and detection of elastic waves in this laboratory. The equipment which has been employed in this work was designed for use with piezoelectric transducers, which have normally a high electrical impedance. In trying to generate elastic waves magnetostrictively, however, it is necessary to excite the surface of the transducer with an rf magnetic field. This type of excitation requires a low-impedance resonant circuit, and, consequently, considerable effort has been directed toward the modification of the existing equipment to permit the use of low-impedance circuitry. This effort has not been completely successful because the equipment was designed in such a manner that its modification would require a complete redesign. Consequently, a rather unsatisfactory compromise modification was employed which, although it permitted observation of the desired phenomena, did not permit optimum execution of the experiment. As a result of this inadequacy of the available apparatus, the generation of elastic waves and their subsequent detection was rather inefficient. Thus, signal-

to-noise ratios were indadequate for quantitative measurements, and only the very qualitative results described above could be obtained. New equipment has been ordered, and it will be put into operation during the second year of this program. This new apparatus will permit the quantitative measurement of elastic-wave amplitudes, and it will permit reliable determination of the polarization (longitudinal or transverse) of the waves.

It is clear from the limited data which have been obtained that single-crystal transducers of the rare earths can, as expected, be used as magnetostrictive elastic-wave transducers.

V. THEORY OF MAGNETIC AND MAGNETOELASTIC RESONANCE IN THE RARE EARTHS

Many attempts to explain magnetic and magnetoelastic phenomena, particularly dynamical phenomena such as magnetic resonance, in terms of theories which had been developed for and applied to iron-group magnetic materials have not met with complete success. Even the calculation of some of the equilibrium characteristics of the rare earths, such as the temperature dependence of the interlayer turn angle in the helimangetis phase, has not proved successful when the special properties of the rare earths are not taken properly into account. As an example, calculations of the field and temperature dependences of uniform-precession ferromagnetic resonance in dysprosium by Cooper and Elliott[35] are not at all in agreement with the observed resonance characteristics reported by Blackstead and Donoho[33]. Nor do the predictions of Cooper and Elliott agree at all with the very sharp, strongly angular-dependent, resonances observed in the helimagnetic phase by Blackstead and Donoho. In the case of elastic-wave propagation and generation, it is virtually impossible to use existing theories to explain any of the phenomena observed in the work reported here, except, as observed in Section III, for the model-independent features of the elastic-wave velocity and attenuation near a magnetic phase transition.

In an attempt to explain some of the observations made

in the course of the experimental work reported here, it became evident a major approximation which has been made in most calculations of dynamic magnetic properties in the iron-group materials is totally inappropriate in the case of the rare earths. This approximation, in which the energy associated with the magnetocrystalline anisotropy is approximated in terms of an effective internal magnetic field, is valid only at temperatures well below the Curie temperature, and it is valid only when the anisotropy energy is a very small fraction of the exchange energy. Consequently, a new theoretical treatment of the magnetic and magnetoelastic properties of the rare earths is under development, and, although detailed calculations have not yet been completely carried out, the preliminary results obtained from this treatment indicate that several phenomena previously unexplained or poorly explained by earlier theories will be in good agreement with the predictions of this new and more accurate theoretical analysis of these problems.

Since the theory is still under development, only the broadly applicable qualitative features are discussed here. However, from the limited discussion which follows, the differences between the present treatment and the treatments which preceded it will be apparent, and the range of applicability of the new theory will be evident. In particular, the applicability of the new theory to the following types of problem,

which are pertinent to the experimental part of this program, is emphasized in this report:

1. Equilibrium magnetic and magnetoelastic properties:

By treating all the contributions to the magnetic and elastic free energy of a rare-earth material simultaneously, regarding the usual magnetic contributions, the exhange and Zeeman energies, on the same level as the crystalline anisotropy and the magnetoelastic energy, it is possible to calculate the equilibrium magnetization, the phase-transition temperatures, the equilibrium magnetostriction, and the helimagnetic interlayer turn angle to greater accuracy than was possible in earlier work. The reason for the better agreement which can be expected between the theory and the experimentally determined equilibrium values of these quantities is simply that the earlier theoretical treatments regarded such quantities as the crystalline anisotropy and the magnetoelastic coupling as small perturbations to the total energy, which was regarded as primarily due to the exchange and Zeeman energies. Yet, in the rare earths, the uniaxial anisotropy energy is as large as one-half the value of the exchange energy, and the magnetoelastic energy is, in some cases, as large as the anisotropy energy. Perturbation treatment of these quantities can, as shown below, lead to serious mistakes in the calculation of equilibrium properties.

2. Magnetic resonance and spin-wave resonance:

All earlier theoretical treatments of spin-wave dispersion relations and the field and temperature dependences of resonance conditions have made what appears to be a seriously invalid approximation in the case of the rare earths. This approximation consists of the replacement of a single-ion type of energy such as the uniaxial anisotropy by a term which is equivalent to the Zeeman energy of an ion in an effective field chosen to give an energy of the same value. This approximation is probably valid in the case of small anisotropy at temperatures far below the Curie temperature in a ferromagnetic material, where each ionic magnetic moment is strongly aligned with the net magnetization by the strong exchange interaction. At higher temperatures, however, the behavior of an ion subjected to the crystalline electric field responsible for the anistotropy is totally unlike that of an ion placed in a magnetic field. As a result of this widely used approximation, the calculated spin-wave properties of rare-earth magnetic materials, which depend strongly on the nature of the rather large anisotropy found in these materials, are probably considerably in error. The previous statement was not more strongly made because few spin-wave measurements have as yet been reported; comparisons with existing theory are, therefore, limited at this time. It is not, however, difficult to see, as shown in what follows, that a more exact

which does not make the "effective-field" approximation, will lead to results that are quite different from the results which are usually obtained using this approximation.

3. Elastic-wave generation and propagation:

Most previous theories have generally made only the crudest approximations in order to find the coupling between spin waves and elastic waves. Normally, the propagation characteristics of each type of wave are calculated separately, and a coupling interaction, usually phenomenological in nature, is introduced, leading to the usual coupled-wave phenomena which are common to all types of wave coupling. In particular, the effects of coupling to the magnetic part of a crystalline system on the propagation of elastic waves have usually been treated in terms of the scattering of these waves by a weak potential whose effects were strong only near a magnetic phase transition (cf. Section III). Yet, in the case of the rare earths, which are strongly magnetostrictive, there are strong coupling mechanisms which are totally unrelated to those which have been previously treated and which lead to strong effects far from the transition temperatures (both above and below). Conventional theories of the dynamical magnetic, elastic, and magnetoelastic properties of solids do not, however, provide a ready quantitative description of the coupling between the magnetic moments and elastic waves. They cannot, therefore, provide

a satisfactory treatment of this coupling in terms of the known equilibrium properties. Rather, the usual theoretical approach is to treat the coupling in terms of a phenomenological interaction whose relationship to the known static properties of the materials cannot be traced. The present theory attempts to get around this difficulty by deriving the coupled equations of motion from a consistent approach which leads to the introduction of no adjustable parameters whose sole purpose is the explanation of one particular set of phenomena. As stated above, however, the theory is still under development, so that only a brief description is presented here. This description will suffice, however, to show how the present treatment leads to a self-consistent picture of all the magnetic, elastic, and magnetoelastic properties, both static and dynamic, of the rare earths.

A. Calculation of Equilibrium Properties

A somewhat simplified model is presented here, for the sake of clarity. The essential features are retained, however, and the model can readily be extended to a more realistic situation characteristic of the actual rare earths. Here, it is assumed that the angular momentum, J, per ion is equal to 1 (Planck's constant, h, is assumed to be unity or otherwise incorporated into other parameters). It is further assumed that the system of interest consists of an assembly of such ions, coupled by exchange

interactions of the isotropic Heisenberg type and that each ion is subject to an axial crystalline electric field which leads to an easy plane of magnetization perpendicular to the anisotropy axis. The magnetoelastic interaction and elastic energy are ignored in this example. They lead to no qualitative difference from the discussion given here. The major point to be made here is the fact that the anisotropy associated with the crystalline electric field cannot be treated accurately in terms of an effective magnetic field even in the calculation of the equilibrium magnetization and other equilibrium properties. For the purpose of this example, the magnetization will be calculated on the basis of the molecular-field model of the exchange. Thus, the Hamiltonian of a single ion becomes

$$\mathcal{H} = g\mu_B \Gamma M J_z - \frac{P_2}{2} (J_x^2 - J_y^2) + (J_z^2 - 2/3) \quad , \qquad (4)$$

where g is the Lande factor, μ_B is the Bohr magneton, Γ is the molecular-field constant, M is the magnetization, and P_2 is a constant representing the strength of the crystalline electric field. The z-axis is the axis of spontaneous magnetization, perpendicular to the anisotropy axis. The energy levels of this Hamiltonian can be found exactly, and the spontaneous magnetization can then be found by means of a straightforward calculation of the expectation value of the magnetic moment, which is equal to the reduced magnetization in magnitude. From this calculation,

the Curie temperature can be obtained, together with the complete temperature dependence of the magnetization. One interesting outcome of this calculation, taking the anisotropy energy explicitly into account in the calculation, is the result that the free energy is a function of temperature even in the paramagnetic region above T_C. Furthermore, the Curie temperature depends strongly on the value of the anisotropy constant, increasing with increasing P_2 until the anisotropy energy is approximately one-half the exchange energy. For large values of P_2, the Curie temperature decreases in this J = 1 case, although this behavior is not significant in the case of the rare earths, which all have much higher J-values. The effective-field approximation for the anisotropy replaces the anisotropy terms in Eq. (4) by another Zeeman term, with an effective field adjusted to give the same value for the energy at T = 0. This approximation, which does not even give the correct single-ion energies, differs strongly from the exact results, particularly as the anisotropy is increased.

If the magnetoelastic energy and the elastic energy are included, in order to find the equilibrium magnetostriction, the problem, for J = 1, is still exactly soluble within the molecular-field approximation (not to be confused with the effective-field approximation, the molecular-field approximation is much better and much more readily justified theoretically). In this case, the

results for the magnetostriction in the easy plane are qualitatively the same as those for the effective-field approximation, but the results for the axial magnetostriction are quite different, in that the effective-field approximation leads to no axial magnetostriction, whereas the exact solution predicts an axial magnetostriction comparable to the planar magnetostriction, in agreement with experimental observations for the rare earths.

Work is in progress to carry out detailed calculations for the case of rare earths with higher J-values and with all the anisotropy and magnetoelastic terms appropriate to these materials. In principle, this exact calculation can be carried out for all realistic cases, but the numerical complexity increases rapidly as J increases, so that the effort at present is being directed toward a generalized calculation using a large-scale computer.

B. Calculation of Dynamic Magnetic and Magnetoelastic Properties

A widely used method for the calculation of the dynamic properties of a quantum-mechanical system involves the use of the Heisenberg equations of motion, in which the time derivative of the expectation value of a quantum-mechanical operator is related to the expectation value of its commutator with the Hamiltonian operator for the system in the following way:

$$\langle \dot{F} \rangle = i \langle [\mathcal{H}, F] \rangle \qquad (5)$$

These equations of motion, when evaluated for all dynamical variables in the system of interest, can often be used to explain the overall dynamical behavior of a system as it deviates from its equilibrium condition. A well-known example is the derivation of the famous Bloch Equations for nuclear magnetic resonance, which describe the behavior of an elementary magnetic dipole in a magnetic field.

If the equations of motion are worked out for a system described by the Hamiltonian of Eq. (4), however, they are somewhat more complicated than the usual Bloch equations because of the crystalline anisotrop terms in the Hamiltonian. For the case in which J = 1, it is necessary to evaluate eight equations of motion instead of the three which would be needed to describe the motion of a free dipole. These equations of motion are the following:

$$\begin{aligned}
\dot{J}_x &= -\omega J_y + P_2 J_4 \\
\dot{J}_y &= \omega J_x \\
\dot{J}_z &= -P_2 J_6 \\
\dot{J}_3 &= 0 \\
\dot{J}_{12} &= -2\omega J_6 \\
\dot{J}_6 &= 2\omega J_{12} + P_2 J_z \\
\dot{J}_4 &= \omega J_5 - P_2 J_x \\
\dot{J}_5 &= -\omega J_4
\end{aligned} \tag{6}$$

The new operators appearing in the above equations of motion are as follows:

$$
\begin{aligned}
J_{12} &= J_x^2 - J_y^2 \\
J_3 &= J_z^2 - J(J+1)/3 \\
J_4 &= J_yJ_z + J_zJ_y \\
J_5 &= J_zJ_x + J_xJ_z \\
J_6 &= J_xJ_y + J_yJ_x
\end{aligned}
\tag{7}
$$

The abbreviation $\omega = g\mu_B\Gamma M$ has also been employed in the equations of motion.

It should be observed that the equations of motion couple the usual operators, J_x, J_y, and J_z, to the new second-degree operators defined above, in contrast to the case of a free ion with no crystal-field anisotropy. The effective-field approximation mentioned above consists in the approximation of the term involving J_4 in the equation of motion for J_x by the term $2\langle J_z\rangle J_y$. With this approximation, the first of Eqs. (6) becomes

$$
J_x = -(\omega - 2P_2\langle J_z\rangle)J_y \quad , \tag{8}
$$

and the equations of motion for J_x and J_y are no longer coupled to the remaining equations. They can be solved, in this approximation, for the normal frequencies of resonance, just as in the case of the free dipole. These frequencies differ, however, from the correct frequencies which would be found from the solution of the complete set of equations of motion, and the difference between

the two solutions becomes quite large when the anisotropy constant, P_2, is appreciable in comparison with the Zeeman frequency, ω.

The exact solution of the equations of motion given above is in agreement with other exact methods of solution (such as, for example, the diagonalization of the Hamiltonian). In this respect, the equation-of-motion approach introduces nothing new, if only the resonant frequencies of a single ion or paramagnetic assembly of ions are required. When, however, the resonant frequencies of a ferromagnetic assembly of ions is required, so that demagnetization effects and collective effects must be taken into account, the equation-of-motion approach, without making the effective-field approximation, will provide accurate results which should agree well with experimental observations. When magnetoelastic coupling is added to the problem, this equation-of-motion approach makes the solutions of problems involving the propagation or the generation of elastic waves quite straightforward. If the elastic and magnetoelastic energies are added to the Hamiltonian of Eq. (4), then a coupled set of equations of motion involving both the crystal strain variables and the angular-momentum variables can be developed. The solution of this complete set of magnetoelastic equations will lead to the solution of problems in magnetic resonance, elastic-wave propagation, and elastic-wave generation.

Unfortunately, the complete set of coupled magnetoelastic equations of motion leads to a formidable problem in numerical analysis, and solutions have not yet been obtained. It is, however, possible to see, in a rather qualitative fashion, that this approach will lead to agreement with experimental results in all the areas of interest to this work. Results are expected early in the second year of this program.

VI. SUMMARY AND CONCLUSIONS

As indicated in the preceding sections of this report, substantial progress has been made in several areas of research related to the magnetic and magnetoelastic properties of rare-earth materials. The studies of elastic-wave propagation and generation have revealed that the dynamic magnetoelastic interactions are strong at high frequency as well as at low frequency. Single-crystal magnetostrictive transducers have been constructed and successfully used for the generation of high-frequency elastic waves. Progress has been made on a new theory which will explain most of the phenomena which have been observed experimentally. Finally, the capability for growing large single crystals of various rare-earth materials has been developed. With this facility, it will be possible to study the properties of a much wider range of materials.

It is expected that the work carried out in this program will have a bearing on the development of new rare-earth permanent magnet materials in other programs sponsored by ARPA. All of the materials currently of interest as permanent-magnet materials exhibit strong magnetostriction. This magnetostriction will undoubtedly have an effect on the performance of magnets fabricated from these materials, and it is hoped that the fundamental studies of magnetostriction being carried out as a part of this program

will yield information of value in the design of permanent-magnet devices based on these new materials.

REFERENCES

1. P. L. Donoho, F. R. Brotzen, and K. Salama, Semi-Annual Technical Report (2 Nov. 1970 to 1 May 1971), ARPA Order No. 1685, Contract No. DAAH01-71-G-0259.
2. S. Legvold, "Rare Earch Research," Macmillan Co., New York (1961), p. 142.
3. E. M. Savitskii, V. F. Terekhova, I. V. Burov, and O. P. Naumkin, "Rare Earth Research," Gordon & Breach, New York (1965), p. 301.
4. H. E. Nigh, J. Appl. Phys. 34, 3323 (1963).
5. C. D. Graham, J. Phys. Soc. Japan 17, 1310 (1962).
6. E. M. Savitskii, V. F. Terekhova, and V. E. Kolesnichenko, Growth and Imperfections of Metallic Crystals (Ed. D. E. Ovsienko (Consultants Bureau, New York, 1968), pp. 118-123.
7. G. C. Wetsel and P. L. Donoho, Phys. Rev. 139 A, 334 (1965).
8. H. G. Meyer, P. F. McDonald, T. D. Stettler, and P. L. Donoho, Phys. Letts. 24 A, 569 (1967).
9. W. C. Koehler, J. Appl. Phys. 36, 1078 (1965).
10. W. C. Koehler, J. Appl. Phys. 36, 1078 (1965).
11. M. Rosen, Phys. Rev. 174, 504 (1968).
12. W. C. Koehler, J. W. Cable, E. O. Wollan, and M. K. Wilkinson, J. Phys. Soc. Japan 17, 32 (1962).

13. W. C. Koehler, J. W. Cable, M. K. Wilkinson, and E. O. Wollan, Phys. Rev. 151, 414 (1966).

14. M. Rosen and H. Klimker, Phys. Rev. B 1, 3748 (1970).

15. M. Long, A. R. Wazzan, and R. Stern, Phys. Rev. 178, 775 (1969).

16. L. M. Levinson and S. Shtrikman, J. Phys. Chem. Solids 32, 981 (1971).

17. T. J. Moran and B. Lüthi, J. Phys. Chem. Solids 31, 1735 (1970).

18. B. Lüthi, T J. Moran, and R. J. Pollina, J. Phys. Chem. Solids 31, 1741 (1970).

19. H. J. McSkimin, J. Acoust. Soc. Am. 33, 606 (1961).

20. Handbook of Chemistry and Physics, edited by R. C. Weast (Chemical Rubber Co., Cleveland, 1968), 49th Ed., p. B-254.

21. S. B. Palmer and E. W. Lee, Phil. Mag. 24, 311 (1971).

22. K. Kawasaki and A. Ikushima, Phys. Rev. B 1, 3143 (1970).

23. G. A. Alers, Physical Acoustics, edited by W. P. Mason (Academic Press, Inc., New York, 1965), Vol. III B, p. 1.

24. M. Rosen, Phys. Rev. Letts. 19, 695 (1967).

25. K. A. Gschneider, Jr., Solid State Physics, edited by F. Seitz and D. Turnbull (Academic Press, Inc., New York, 1964), Vol. 16, p.

26. K. Tani and H. Mori, Prog. Theor. Phys. 39, 876 (1968); Phys. Letts. 19, 627 (1966).

27. H. S. Bennett and E. Pylte, Phys. Rev. 155, 553 (1967); 164, 712 (1967).

13. W. C. Koehler, J. W. Cable, M. K. Wilkinson, and E. O. Wollan, Phys. Rev. 151, 414 (1966).

14. M. Rosen and H. Klimker, Phys. Rev. B 1, 3748 (1970).

15. M. Long, A. R. Wazzan, and R. Stern, Phys. Rev. 178, 775 (1969).

16. L. M. Levinson and S. Shtrikman, J. Phys. Chem. Solids 32, 981 (1971).

17. T. J. Moran and B. Lüthi, J. Phys. Chem. Solids 31, 1735 (1970).

18. B. Lüthi, T. J. Moran, and R. J. Pollina, J. Phys. Chem. Solids 31, 1741 (1970).

19. H. J. McSkimin, J. Acoust. Soc. Am. 33, 606 (1961).

20. Handbook of Chemistry and Physics, edited by R. C. Weast (Chemical Rubber Co., Cleveland, 1968), 49th Ed., p. B-254.

21. S. B. Palmer and E. W. Lee, Phil. Mag. 24, 311 (1971).

22. K. Kawasaki and A. Ikushima, Phys. Rev. B 1, 3143 (1970).

23. G. A. Alers, Physical Acoustics, edited by W. P. Mason (Academic Press, Inc., New York, 1965), Vol. III B, p. 1.

24. M. Rosen, Phys. Rev. Letts. 19, 695 (1967).

25. K. A. Gschneider, Jr., Solid State Physics, edited by F. Seitz and D. Turnbull (Academic Press, Inc., New York, 1964), Vol. 16, p.

26. K. Tani and H. Mori, Prog. Theor. Phys. 39, 876 (1968); Phys. Letts. 19, 627 (1966).

27. H. S. Bennett and E. Pylte, Phys. Rev. 155, 553 (1967); 164, 712 (1967).

28. H. Okamoto, Prog. Theor. Phys. 37, 1348 (1967).

29. K. Kawasaki, Solid St. Communication 6, 57 (1968).

30. K. Kawasaki, Phys. Letts. 26A, 543 (1968).

31 G. E. Laramore and L. P. Kadanoff, Phys. Rev. 187, 619 (1969).

32. R. J. Pollina and B. Lüthi, Phys. Rev. 177, 841 (1969).

33. H. A. Blackstead, Thesis, Rice University, unpublished (1967).

34. B. R. Cooper, Solid State Physics 21, 356 (1969).

35. B. R. Cooper and R. J. Elliott, Phys. Rev. 131, 1043 (1963).

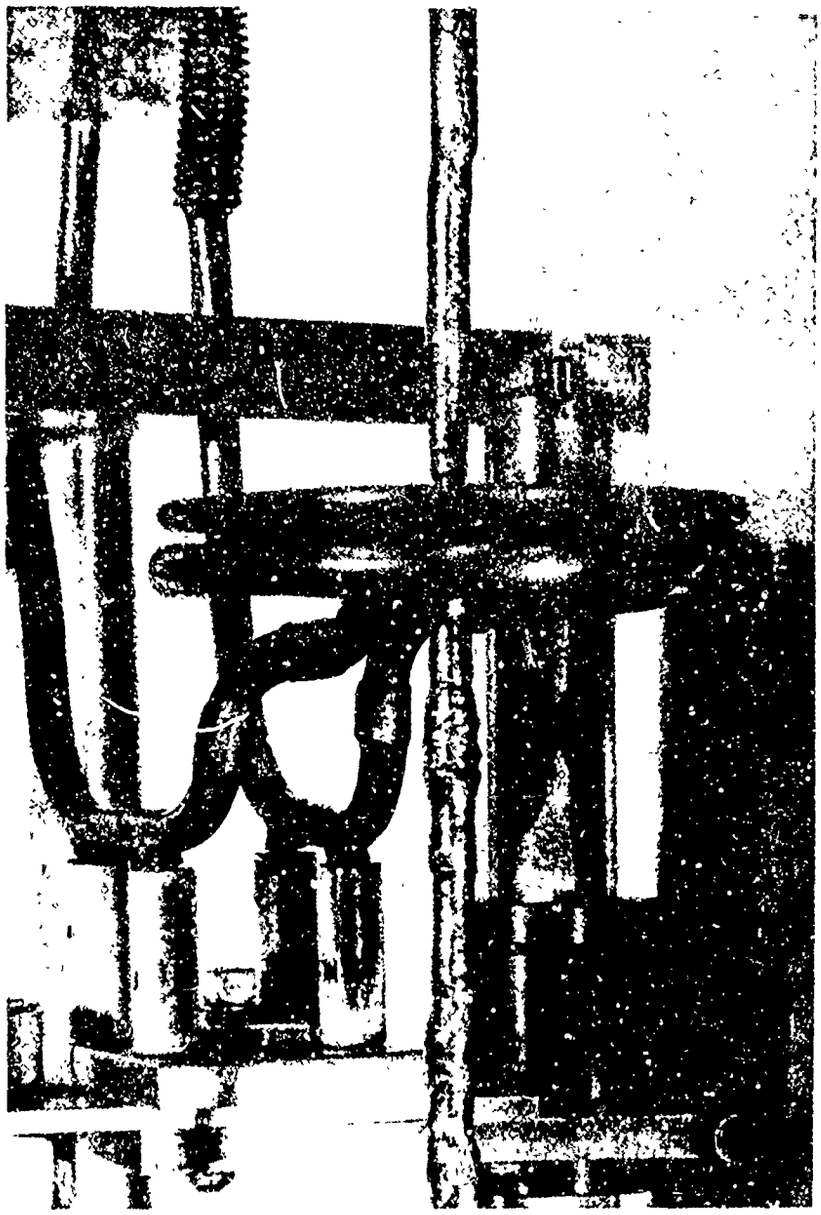

Fig. 1 Induction coil and specimen installed in zone-refining equipment.

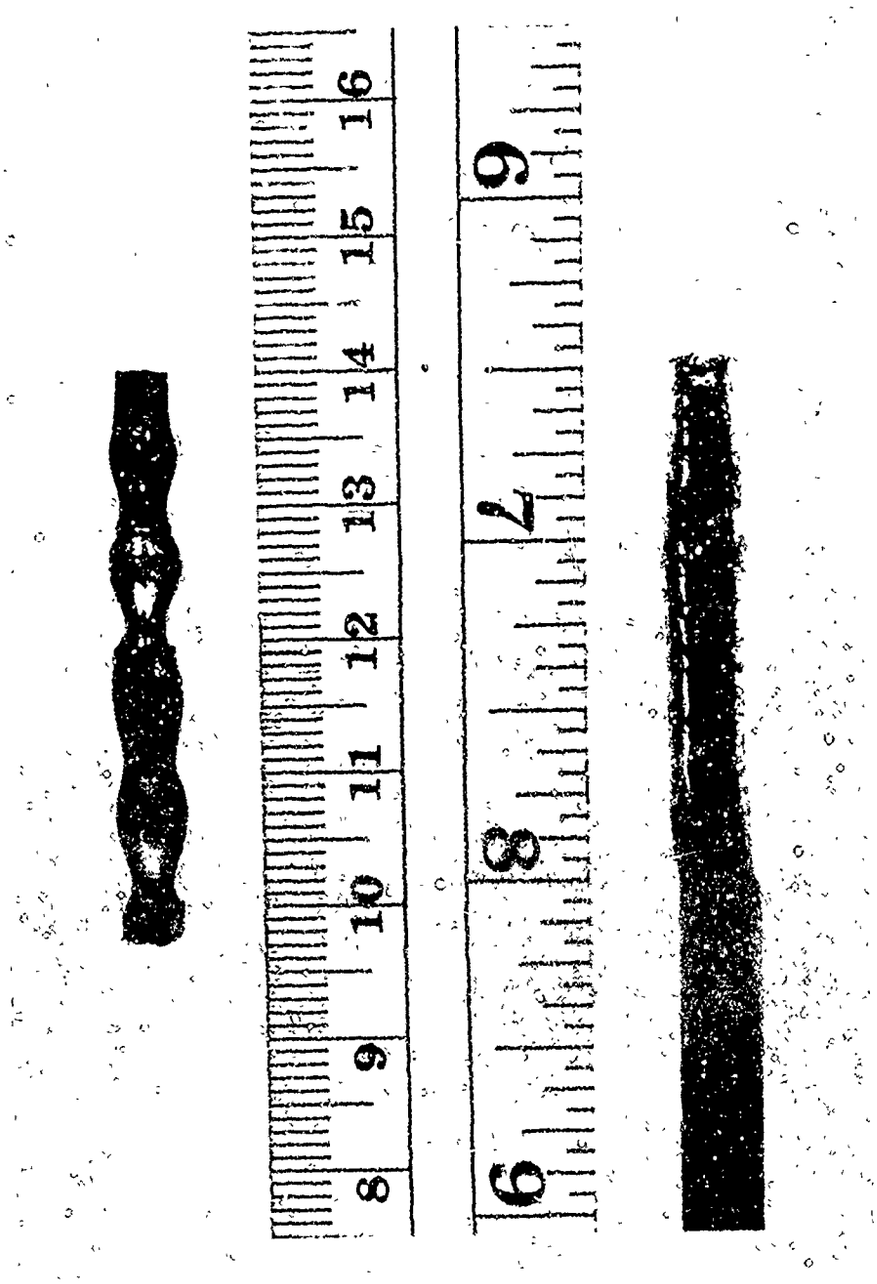

Fig. 2 - Comparison of single crystals grown by floating-zone induction-melting technique with and without satisfactory power control.

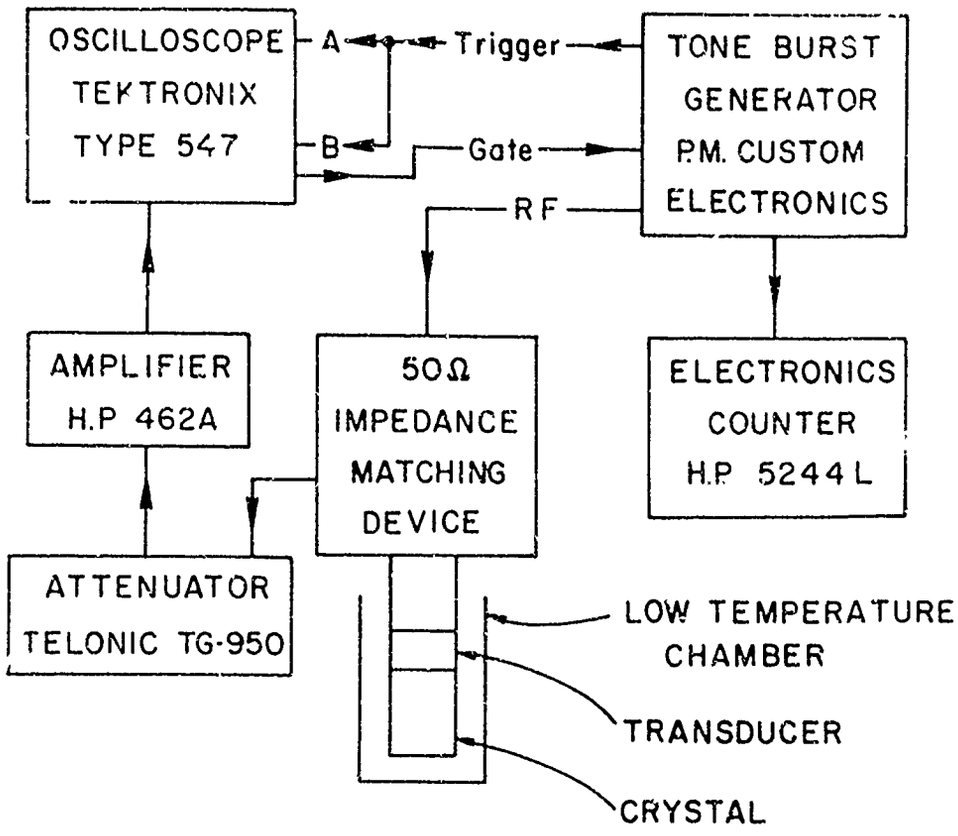

Fig. 3 - Schematic diagram of the experimental arrangement for measuring ultrasonic velocities.

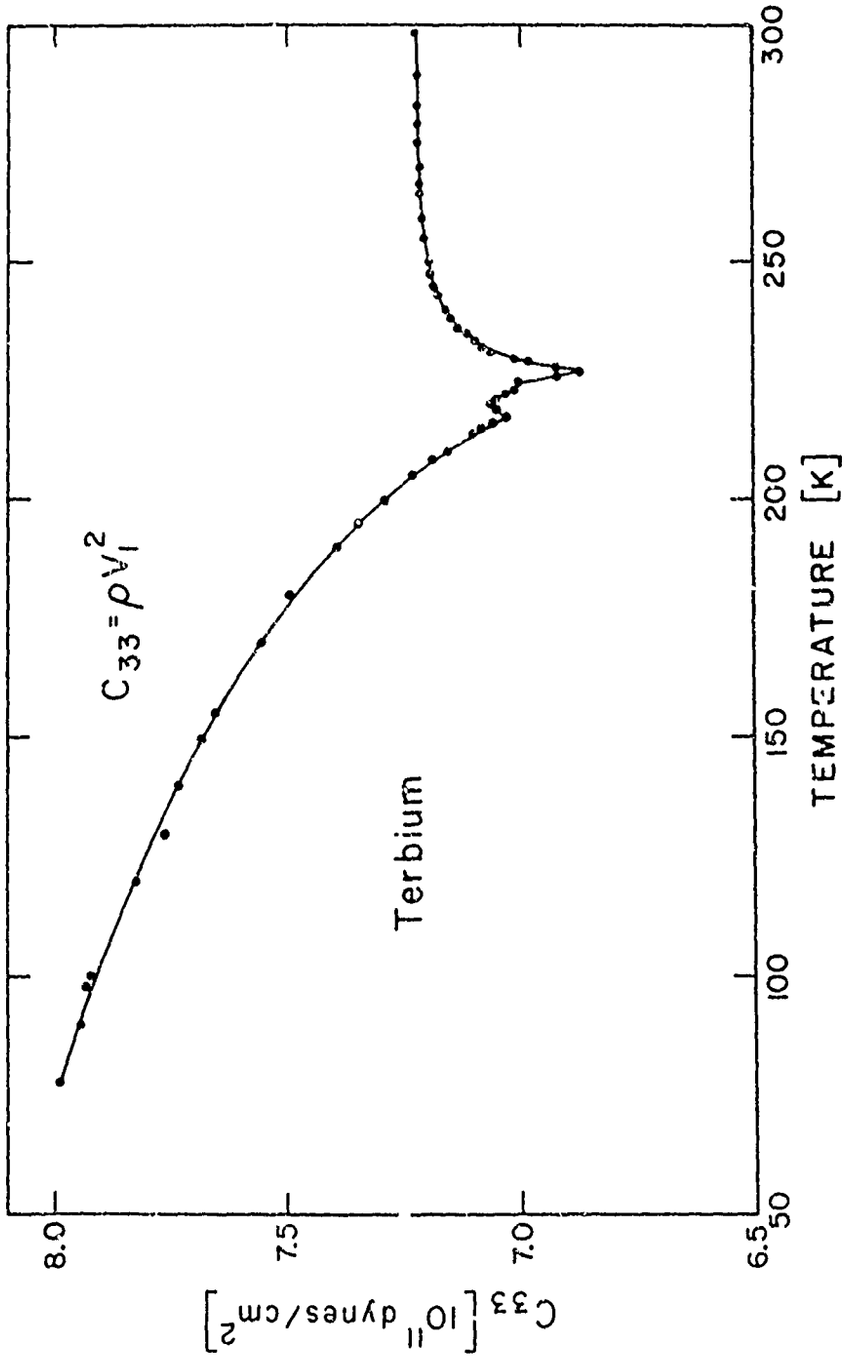

Fig. 4 - Temperature dependence of the adiabatic elastic constant c_{33} in terbium.

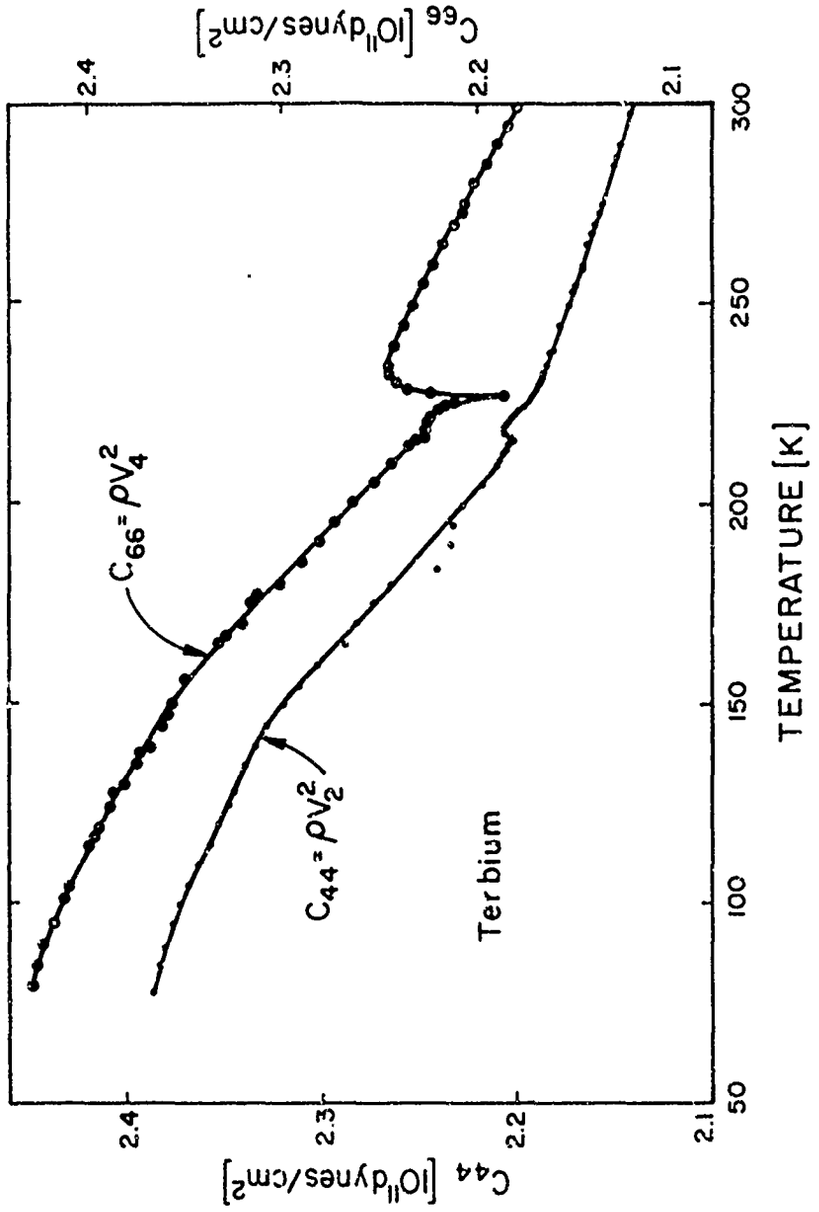

Fig. 5 - Temperature dependence of the adiabatic elastic constants c_{44} and c_{66} in terbium.

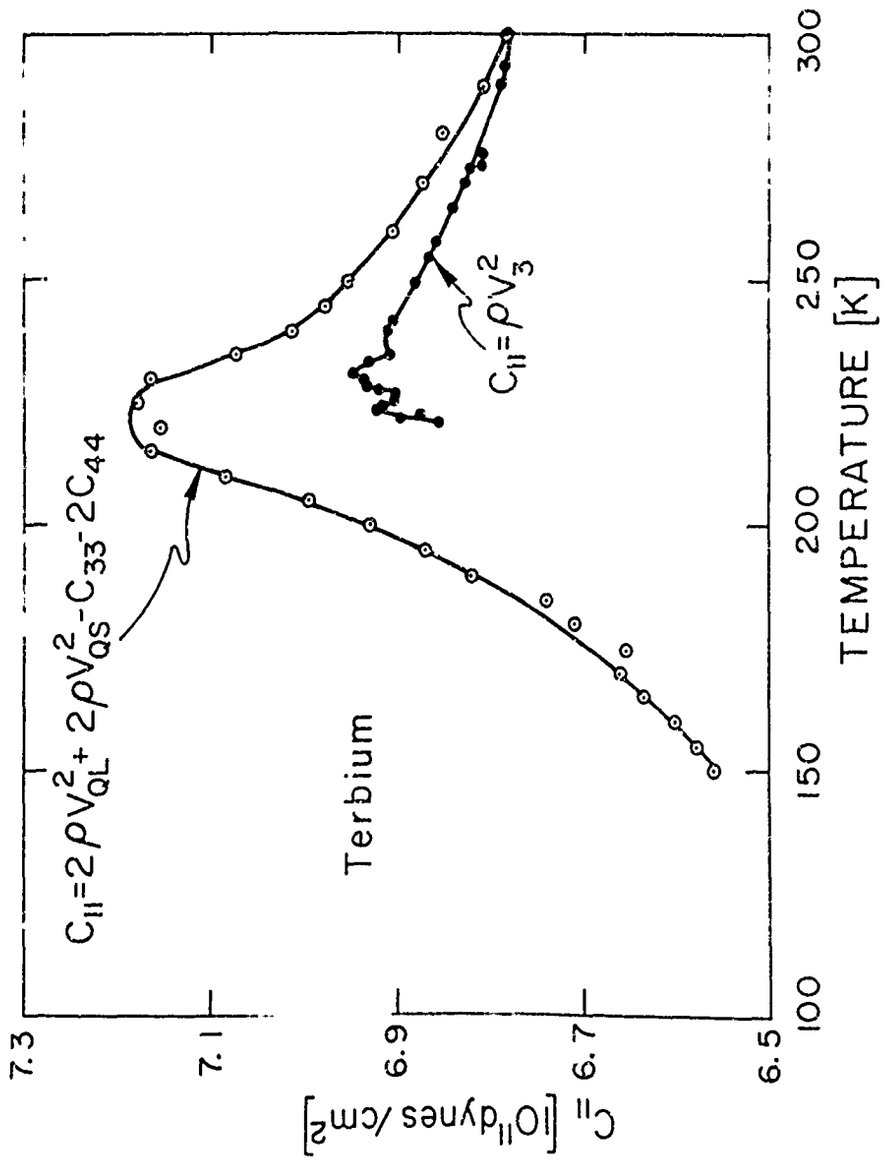

Fig. 6 - Temperature dependence of the adiabatic elastic constant c_{11} in terbium. • determined from a single measurement; ⊙ determined indirectly from four measurements.

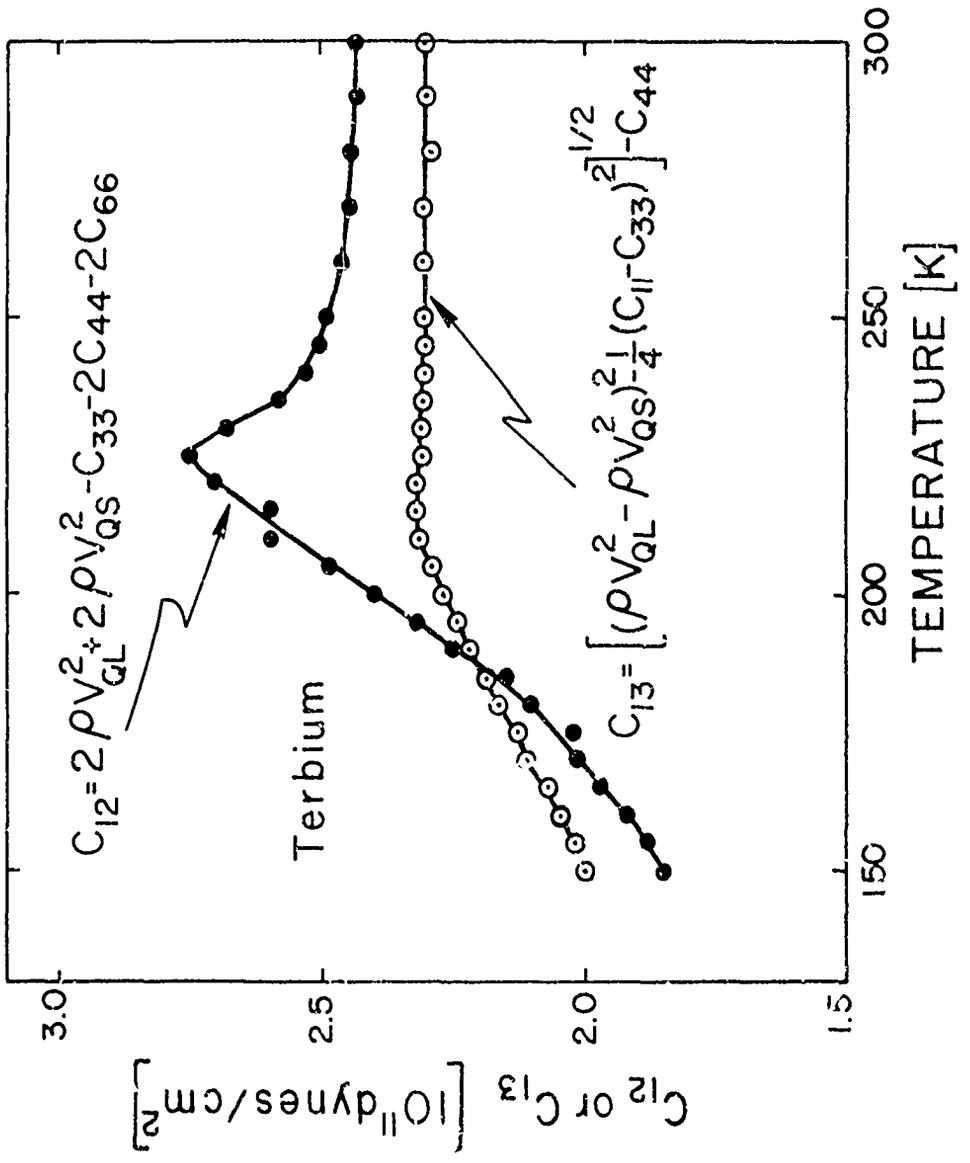

Fig. 7 - Temperature dependence of the adiabatic elastic constants c_{12} and c_{13} in terbium. Both constants were determined from five measurements.

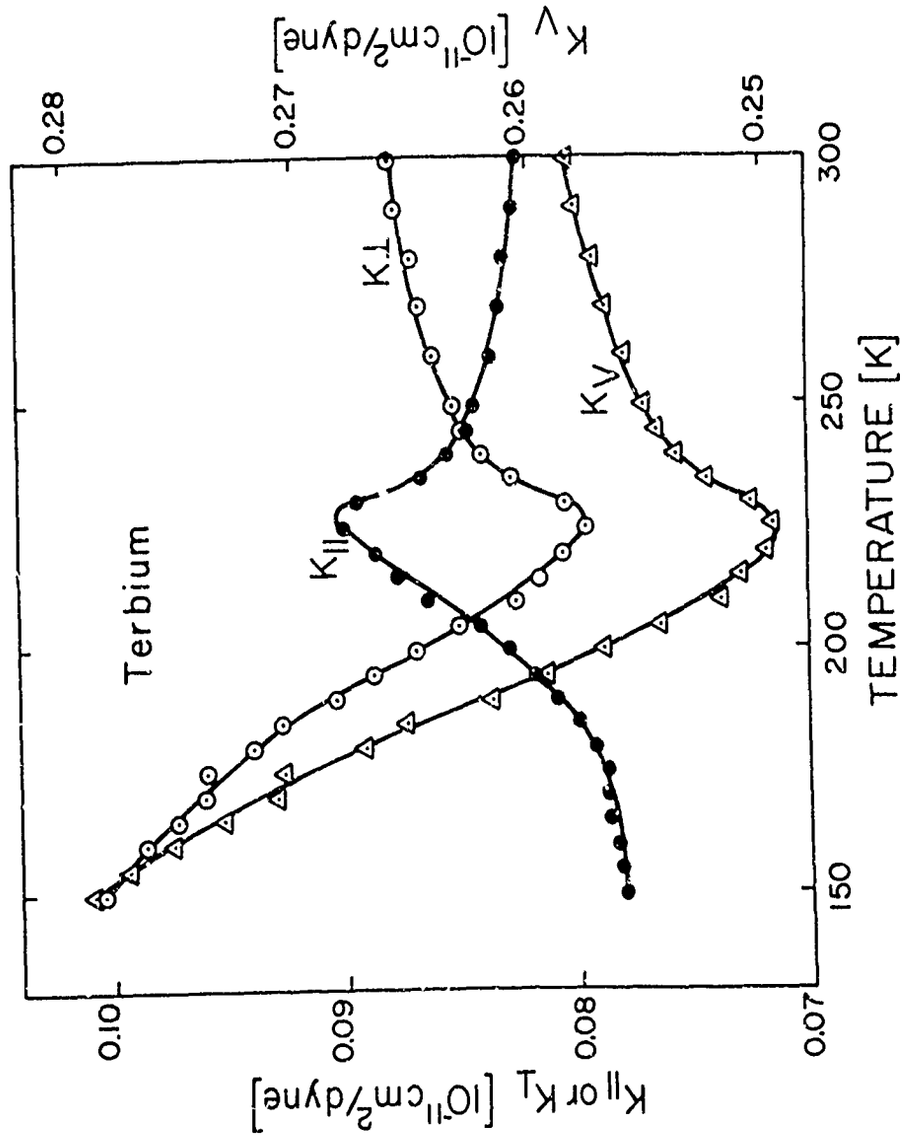

Fig. 8 - Temperature dependence of the parallel ($K_{\parallel}$), perpendicular ($K_{\perp}$) and volume (K_V) compressibilities in terbium. The compressibilities were determined using the relationships in the footnote to Table II.

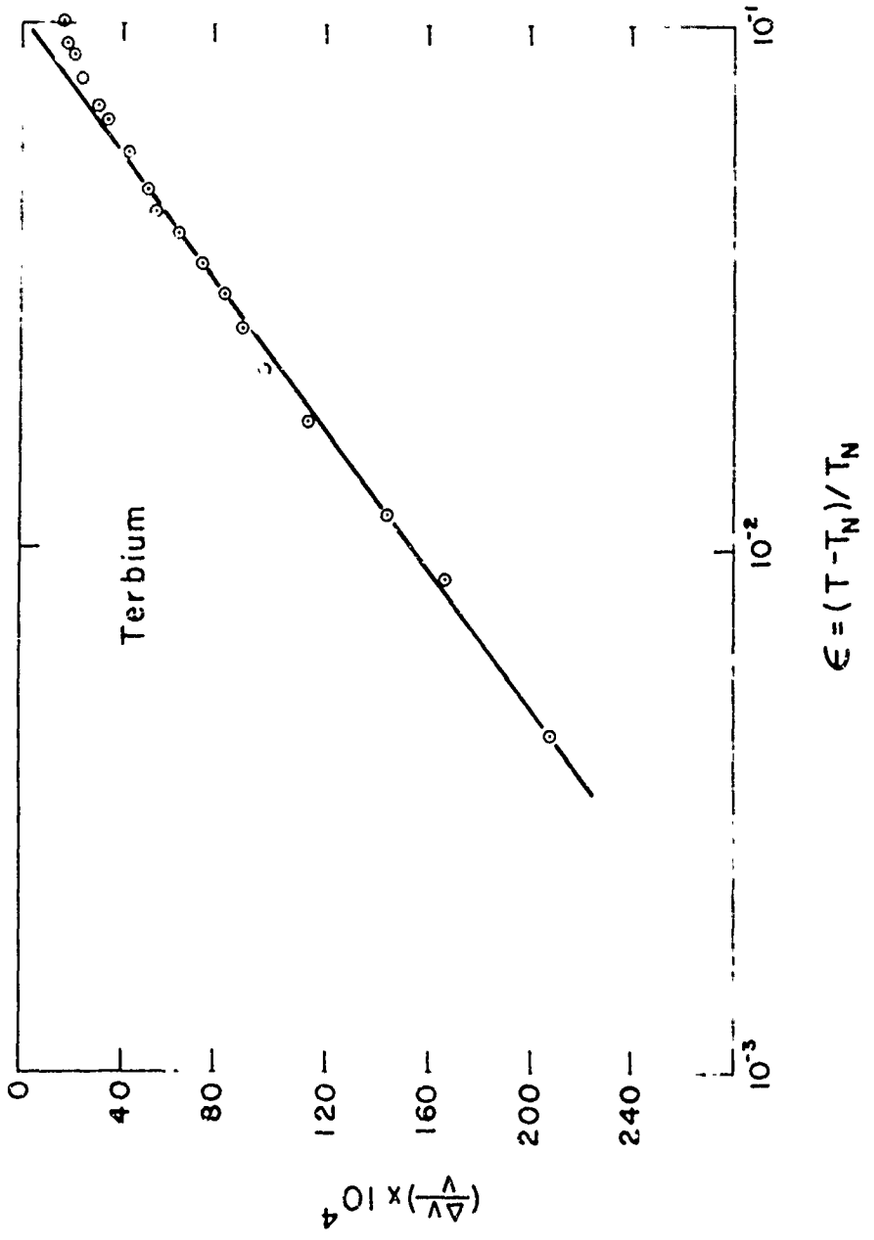

Fig. 9 - Temperature dependence of the relative velocity change of ultrasonic longitudinal wave propagating in the [0001] direction near the Néel temperature in terbium.

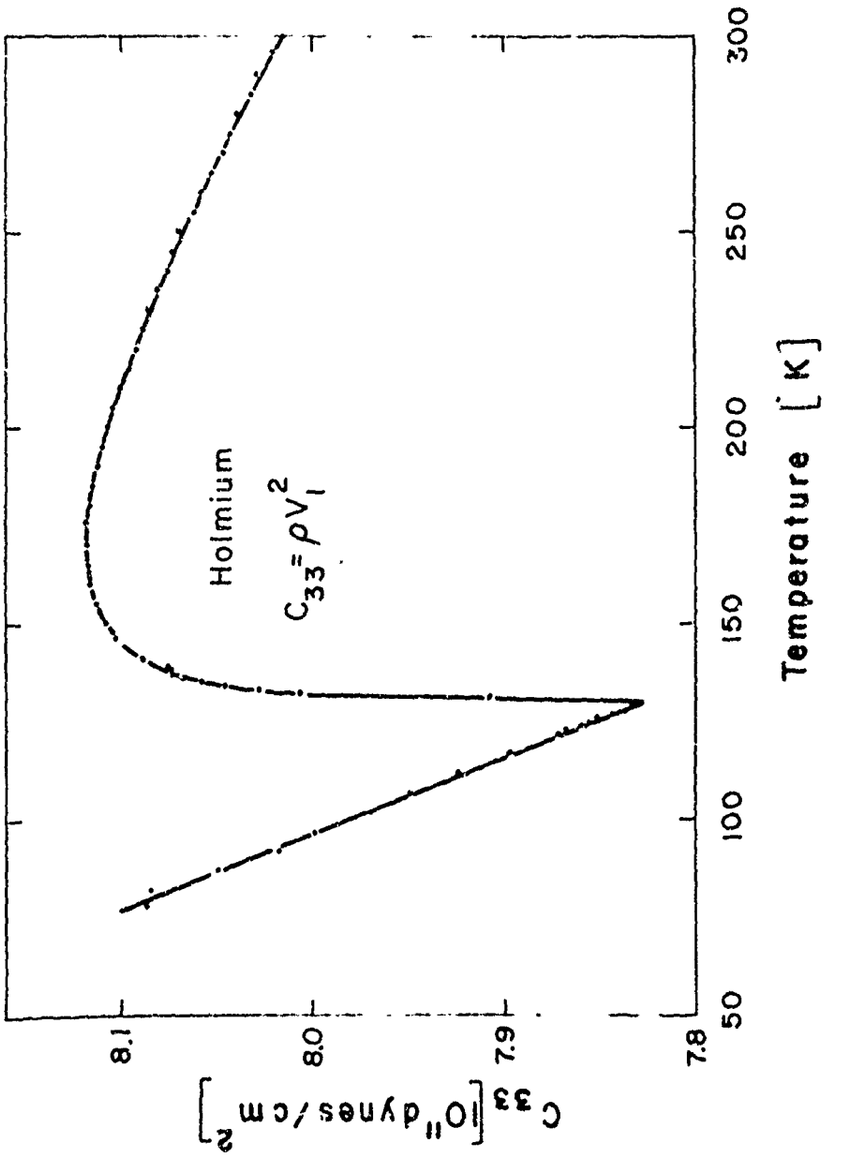

Fig. 10 - Temperature dependence of the adiabatic elastic constant c_{33} in holmium.

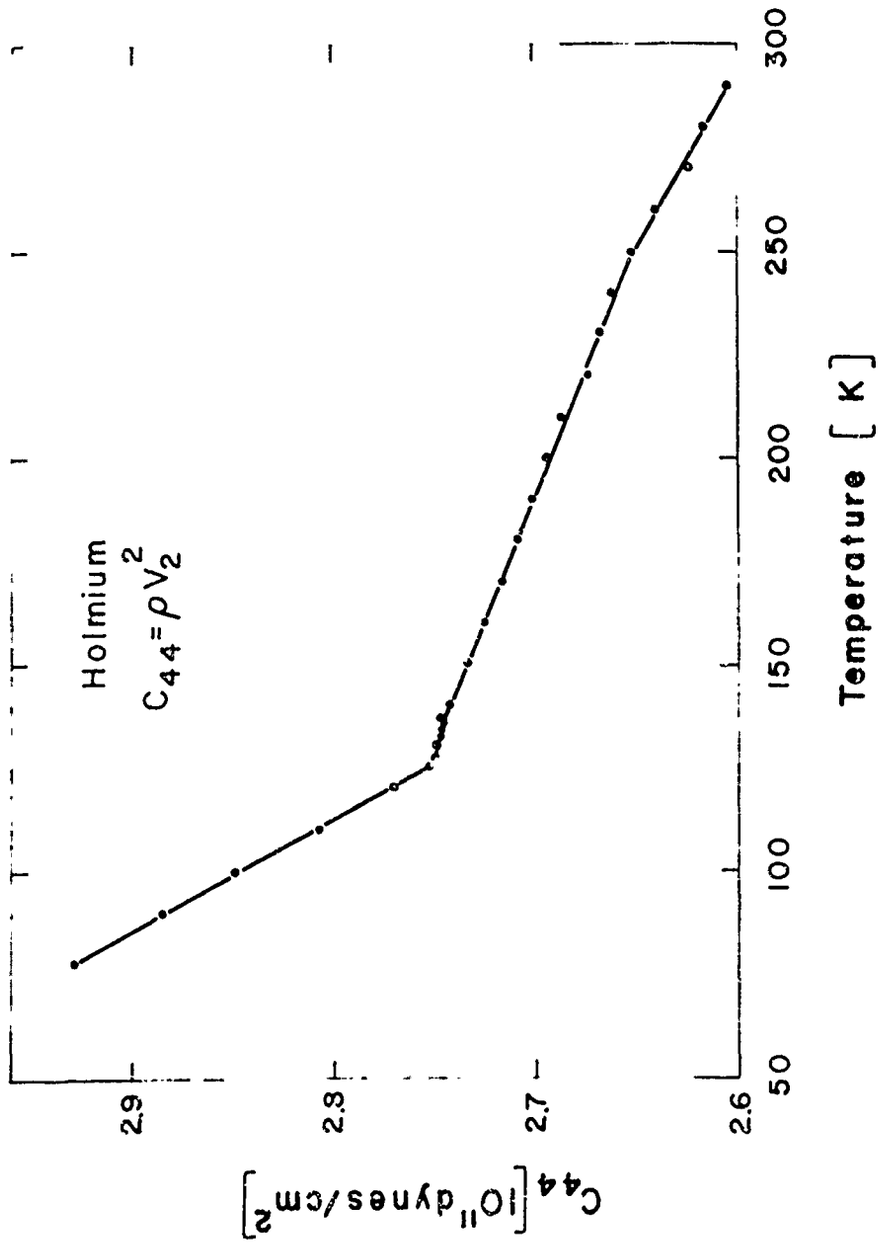

Fig. 11 - Temperature dependence of the adiabatic elastic constant c_{44} in holmium.

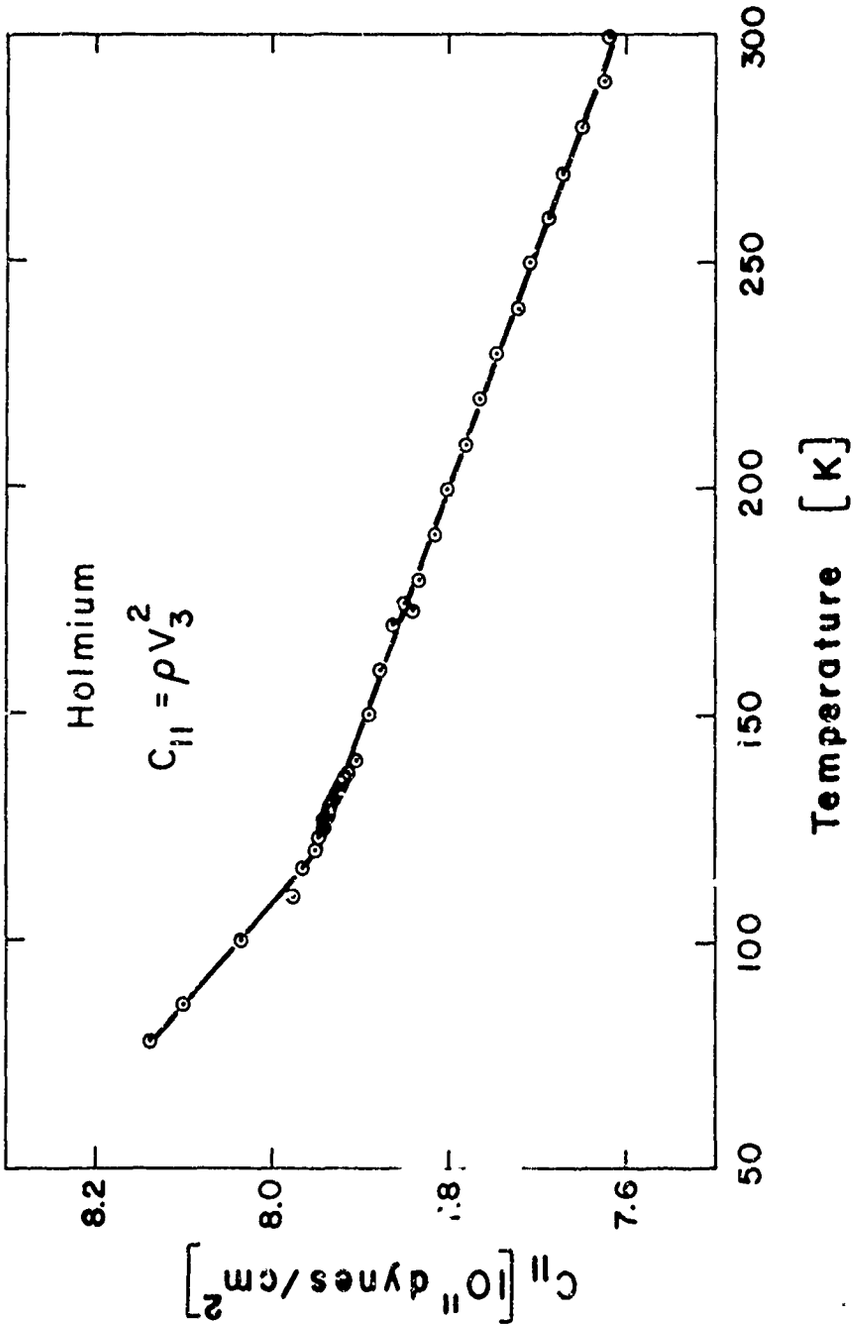

Fig. 12 - Temperature dependence of the adiabatic elastic constant c_{11} in holmium.

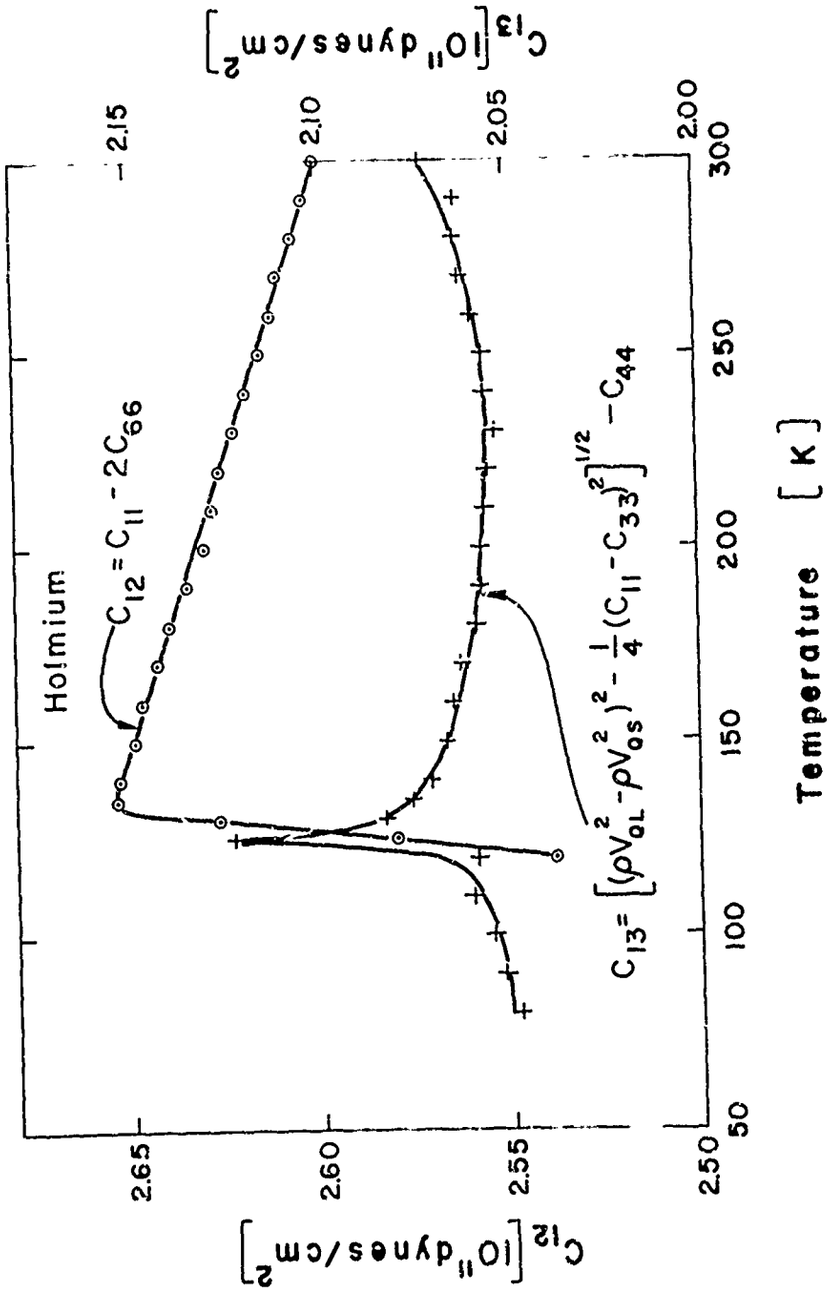

Fig. 13 - Temperature dependence of the adiabatic elastic constants c_{12} and c_{13} in holmium.

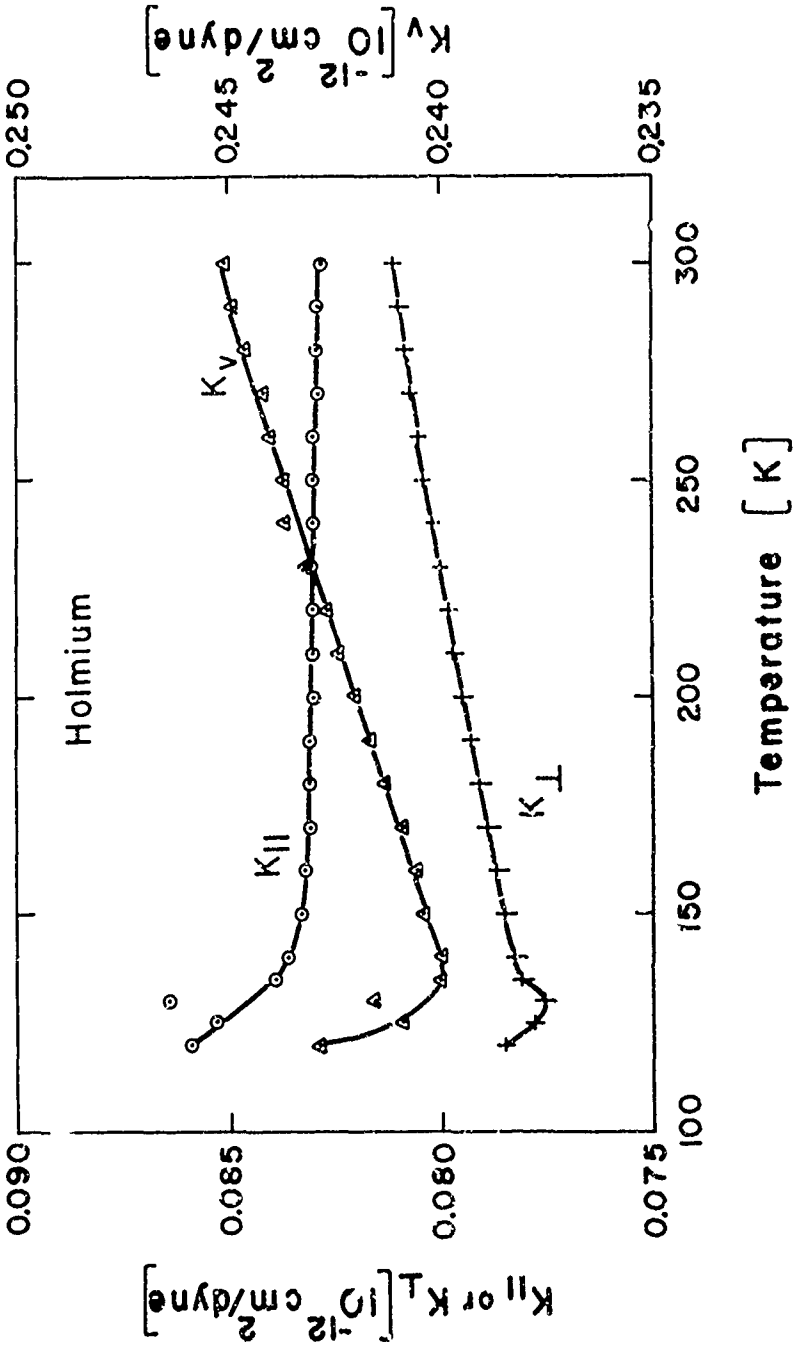

Fig. 14 - Temperature dependence of the directional compressibilities K_{II} and $K_\perp$ and the volume compressibility K_V of holmium.

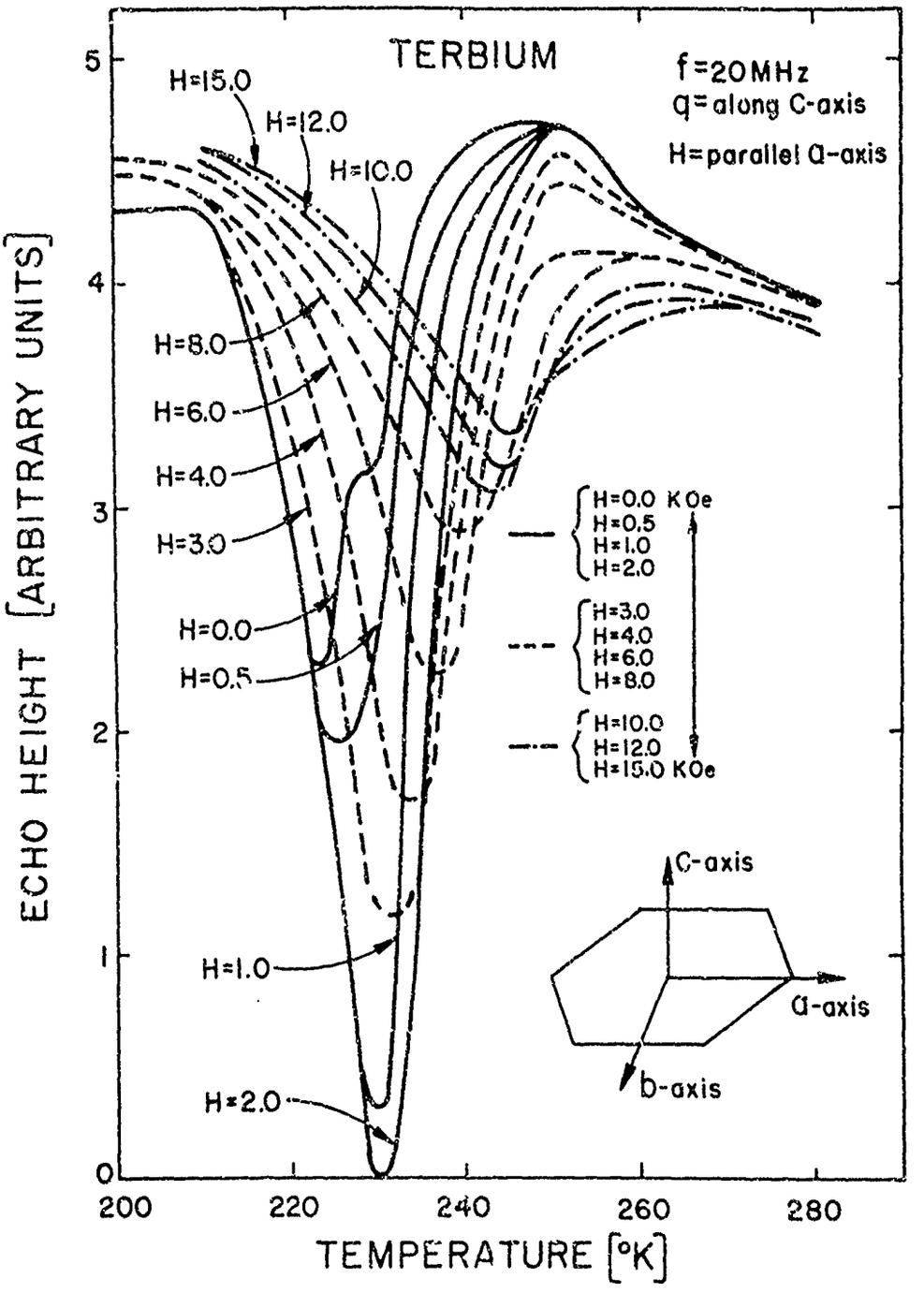

Fig. 15 - Temperature dependence of ultrasonic echo height in terbium single crystals at various applied magnetic fields. Longitudinal waves at 20 MHz propagating along the c-axis and magnetic fields applied in the basal plane parallel to the a-axis.

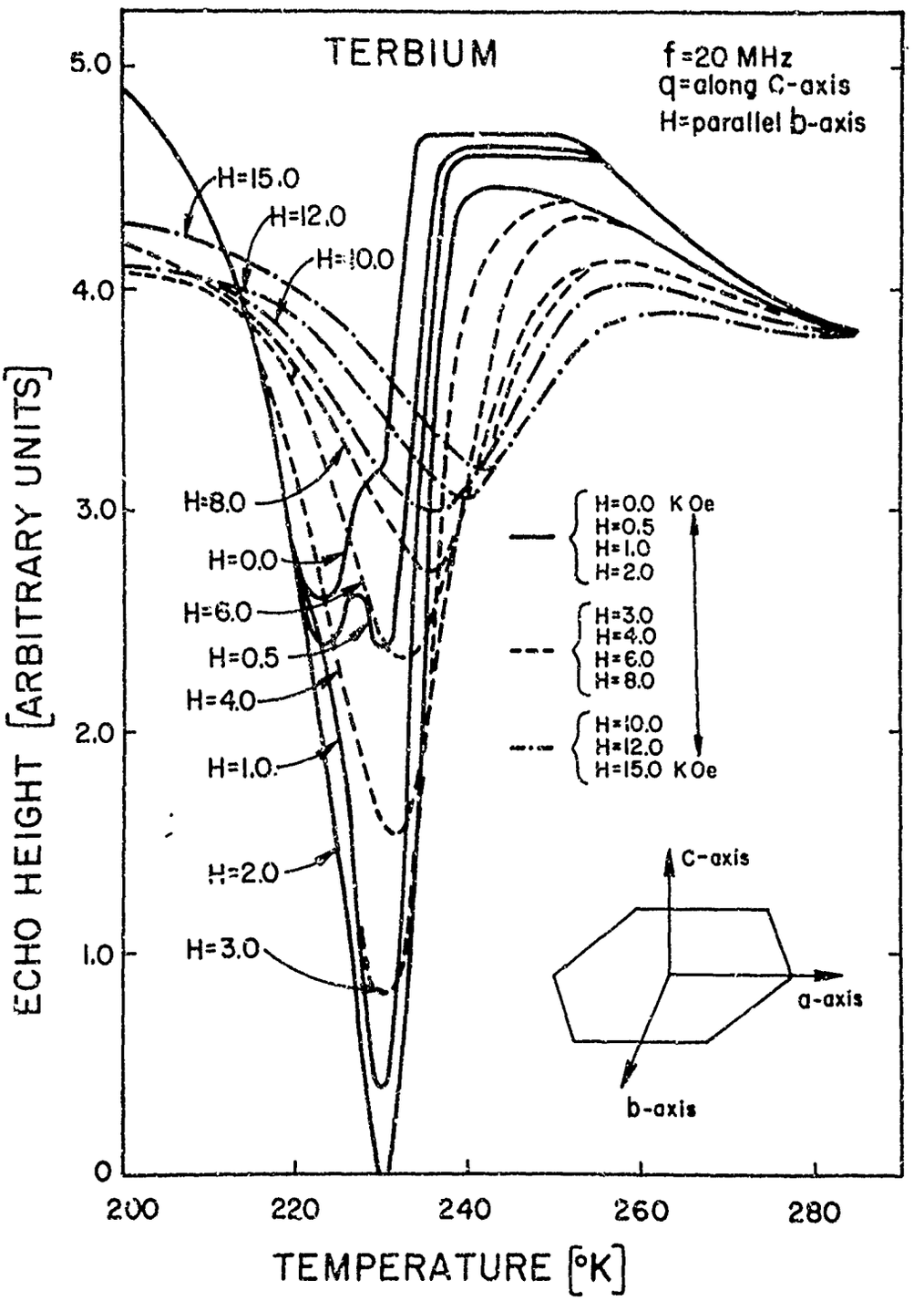

Fig. 16 - Temperature dependence of ultrasonic echo height in terbium single crystals at various applied magnetic fields. Longitudinal waves at 20 MHz propagating along the c-axis and magnetic fields applied in the basal plane parallel to the b-axis.

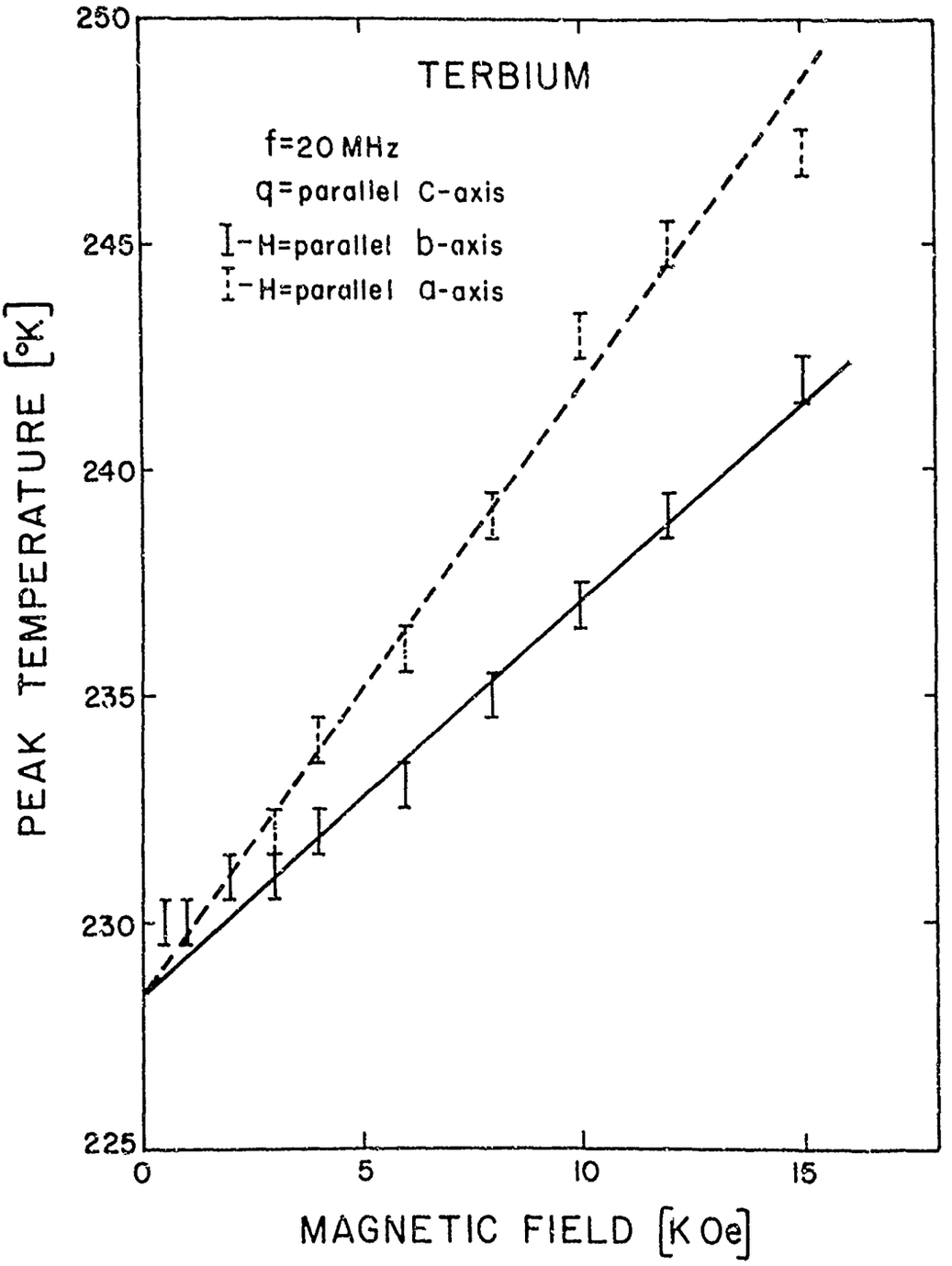

Fig. 17 - Peak temperature of the ultrasonic echo height in terbium single crystals (shown in Figs 27 and 28) versus magnetic field applied in the a- or in the b-axis. The intercept temperature of the two straight lines is 228.5° K.

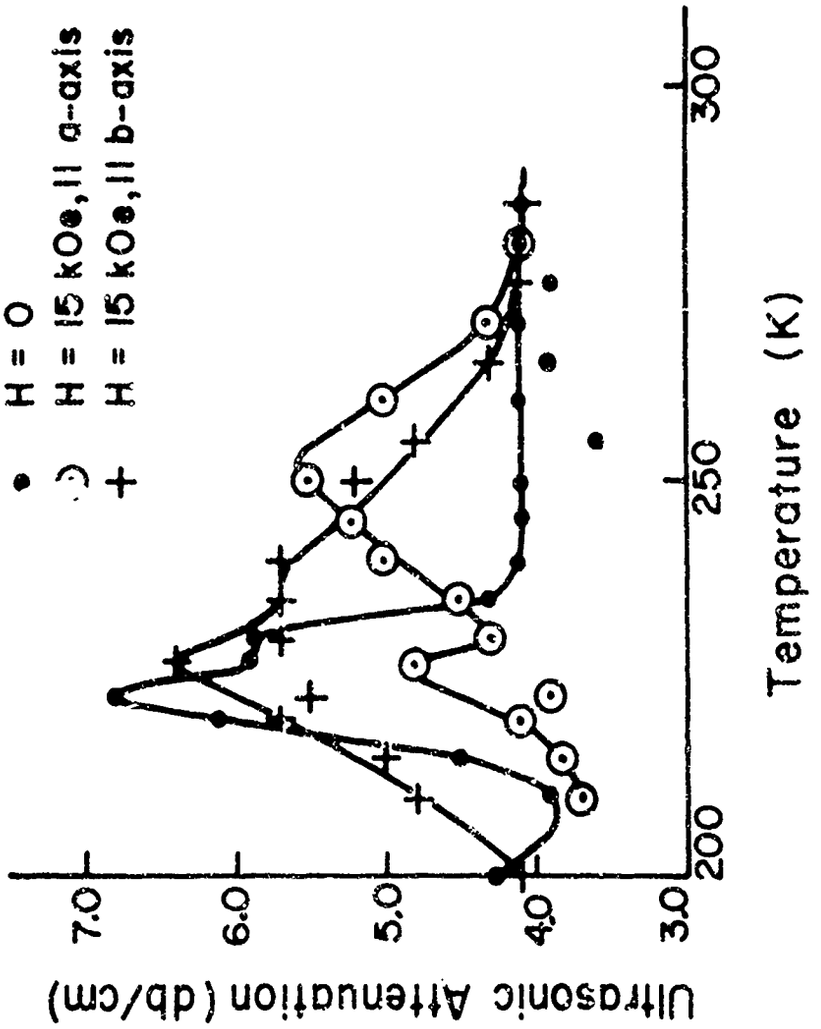

Fig. 18 - Temperature dependence of ultrasonic attenuation in terbium single crystals; longitudinal waves at 20 MHz propagating along the c-axis without and with magnetic field applied parallel to the a- or b-axis.

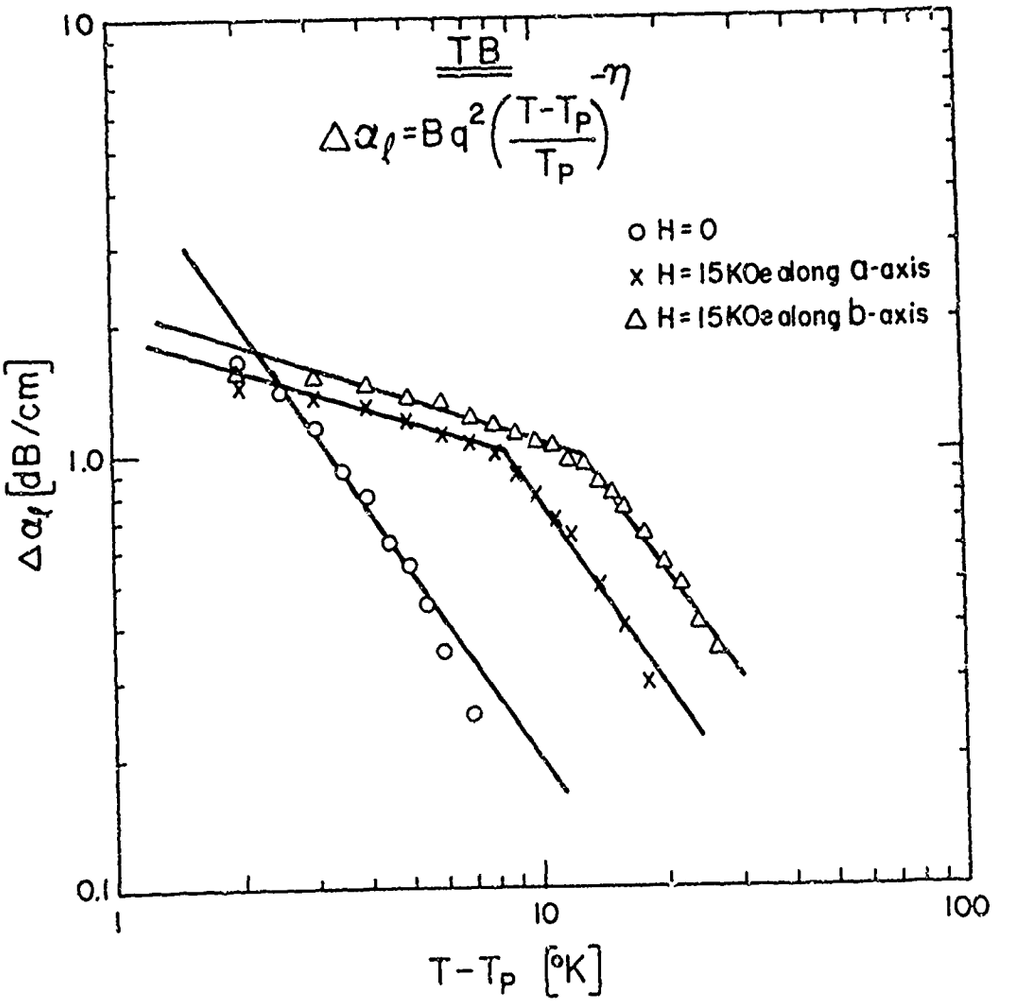

Fig. 19 - Log-Log plot of the critical ultrasonic attenuation in terbium single crystals and temperature. Longitudinal waves at 20 MHz propagating along the c-axis; without and with magnetic field applied parallel to the a- or the b-axis.

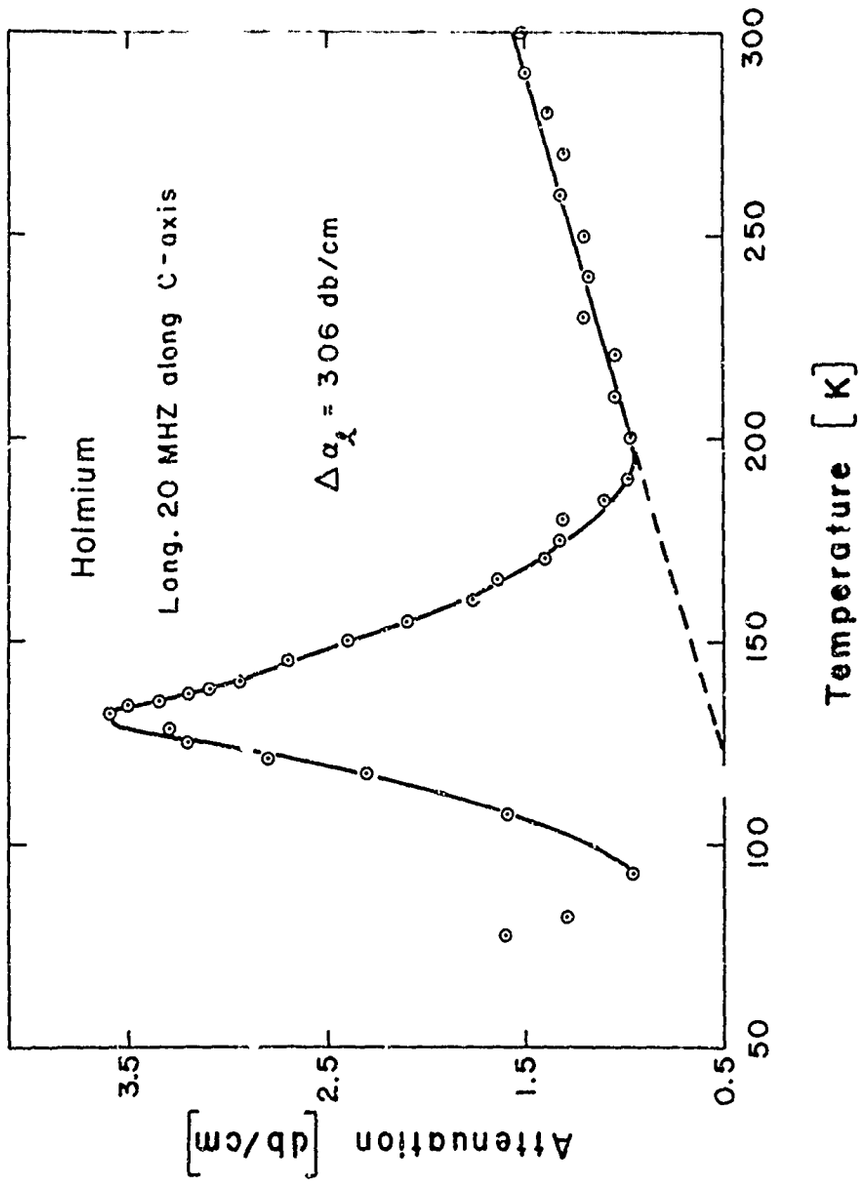

Fig. 20 - Temperature dependence of the ultrasonic attenuation in holmium single crystals; longitudinal waves at 20 MHz propagating along the c-axis.